Application of plasma lenses to the AWAKE interstage

Study of nonlinear effects

Rune Sivertsen

Thesis submitted for the degree of

Master of science in Physics

60 credits

Department of Physics

Faculty of mathematics and natural sciences

UNIVERSITY OF OSLO

Spring 2017

Application of plasma lenses to the AWAKE interstage

Study of nonlinear effects

Rune Sivertsen

Application of plasma lenses to the AWAKE interstage

http://www.duo.uio.no/

Printed: Reprosentralen, University of Oslo

ABSTRACT

A future possible acceleration technique for linear colliders is plasma wakefield acceleration. One of the questions unanswered today is whether we can use this technology to achieve TeV-scale acceleration with a good enough beam quality. The AWAKE-experiment at CERN has as goal to demonstrate the feasibility of TeV acceleration using an SPS proton beam as a plasma driver. For Run 2 of AWAKE we need to self-modulate the proton beam before we inject an electron witness beam in the acceleration stage. This creates a interstage between the two plasma cells, where the proton beam needs to be refocused in a limited space.

We have looked at plasma lenses as a solution to this problem, since they both deliver stronger magnetic fields and have axisymmetric focusing compared to conventional magnetic quadrupoles. We have in particular studied nonlinear effects; nonlinear magnetic field due to non-uniform current distribution, and wakefields originating from the charged beam being focused. In a relation to a pre-study of plasma lenses at the CLEAR-facility at CERN, we have studied where the wakefield is significant, in preparation for further experimental verification at CLEAR.

We have then studied whether plasma lenses can be used for an AWAKE interstage. The results with and without nonlinear effects are the same: to use plasma lenses we need improved plasma lenses with respect to today's state of the art. However, assuming higher current and longer lenses than available today, plasma lenses could potentially be interesting for the AWAKE interstage.

ACKNOWLEDGEMENTS

When I started my masters, I had originally thought about working with dark matter or nuclear physics. Until a presentation during a trip to CERN about future linear colliders made me interested in the accelerators in itself, and how a more practical approach could be a good direction after a theoretical bachelor. After two years my interest has not dwindled, it has rather increased.

Firstly, I would to express my gratitude to my advisor assoc. prof. Erik Adli, for investing his time in me and for his enthusiasm in this field. I deeply appreciate the discussions about analysis, accelerators and all the different methods to measure the beams. Thank you as well for showing me around at CERN, DESY and ESS, answering all my dumb questions.

Secondly my thanks to two of the PhD students in the HEP-group, Carl Andreas Lindstrøm and Veronica Berglyd Olsen. Without them I would still be sitting debugging the two others simulation codes we tried first. Outside of them, a thank you to my fellow master students Sean Miller, Alocias Mariadason and Alexander Fleischer; for trying to discuss something outside their fields.

My thanks also goes towards two of my teachers before the University, Bjørn Singsaas and Morten Sæther. Without them I would never have started to like physics at all! A thanks as well to the student society Realistforeningen, for never letting me leave the campus after the lectures. And finally, to my twin sister, for always having time at the middle of the night for a talk.

CONTENTS

LIST OF FIGURES

LIST OF TABLES

I. INTRODUCTION

The goal of a particle accelerator is rather simple; accelerate a particle beam to a specific energy while preserving the beam quality as much as possible. Particle colliders smash two beams of particles of high energy together with the aim of studying fundamental particles and interactions of nature. Particle colliders collide either hadrons (protons, anti-protons) which are heavy, composite particles, or leptons (electrons, positrons) which are fundamental particles.

Hadron colliders are often called discovery machines due to their larger energy range, while lepton colliders may often provide more accurate physics . The most effective way to accelerate particles is by circular orbits such that we reuse the accelerating cavities each turn. For electron and positron acceleration, there is an upper limit on the collision energy due to synchrotron radiation loss, which scales as the fourth power of the particle energy.

The highest energy lepton collider to date, to the author′s knowledge, is Large Electron Positron collider (LEP) at CERN, which had a maximum collision energy of 209 GeV. In order to achieve this energy, the tunnel had to be filled with RF cavities as much as possible to compensate for the synchrotron radiation loss. A future electron-positron collider, aiming to reach TeV-scale energies, would be prohibitively large and expensive because of this loss. Even the proposed FCC-ee (Future Circular Collider[1]) at 350 GeV would need to a ring circumference of 80-100 km.

For TeV-scale lepton collisions, linear colliders such as ILC[2] and CLIC[3] are therefore currently proposed. These machines also needs to be somewhat large, with proposed length of 30 km and 50 km respectively, due to limits of accelerating gradient in regular RF-based accelerating cavities. To reach the luminosity targets, the colliding beams in linear colliders also has to be as compact as possible.

Plasma wakefield acceleration is novel acceleration technique where one studies whether the very strong fields that can be set up in plasmas can be used to accelerate particle beams of good quality. If strong enough oscillations in the plasma occur, creating a sufficient local excess of electrons or ions within the plasma, strong electric fields along

the beam axis may be set up. The corresponding accelerating gradients in plasma have been shown to be 10-100 times stronger than for RF-based cavities.

Oscillations like these are called wakes, and corresponding electromagnetic fields are denoted as wakefields. A short, intense laser pulse, or a high energy particle beam, may be used to drive such plasma wakes. The witness beam can then be placed in the wake of the driver, and "ride" the accelerating field.

If the oscillations are small, the plasma wake is in the linear regime, meaning that the fields set up are proportional to the drive beam current. If the drive beam current is stronger, all the plasma electrons trailing a drive beam may be expelled from the beam axis, and the wake is said to be in the blow-out regime, sometimes called the bubble regime.

The idea to accelerate particles with plasmas was proposed already in 1979[4]. At that time with a laser pulse method, where the acceleration was calculated to be of several orders higher than conventional radio-frequency acceleration used today. In 2014 FACET at SLAC published proof of principle[5] of accelerating particle beams with very high gradients, for a small plasma stage and with an electron beam as both the driver and witness of the wakefield.

Future lepton colliders should ideally collide particles at the TeV-scale. In order for an electron beam driven (or laser driven) plasma accelerator to achieve this, many electron drive beams (or laser drive pulses) would be needed, each driving a single plasma stage, because the total energy in existing electron bunches is much less than what is needed to produce a high-charge TeV-bunch.

Another approach is to use the available high-energy proton bunches at CERN, the SPS beam and the LHC beam, to drive the plasma instead. With an LHC-beam, a high-charge electron bunch could in principle be accelerated to TeV-scale in a single plasma acceleration stage[6][7]. The objective of the AWAKE experiment at CERN is to study such a proton beam driven plasma wakefield acceleration.

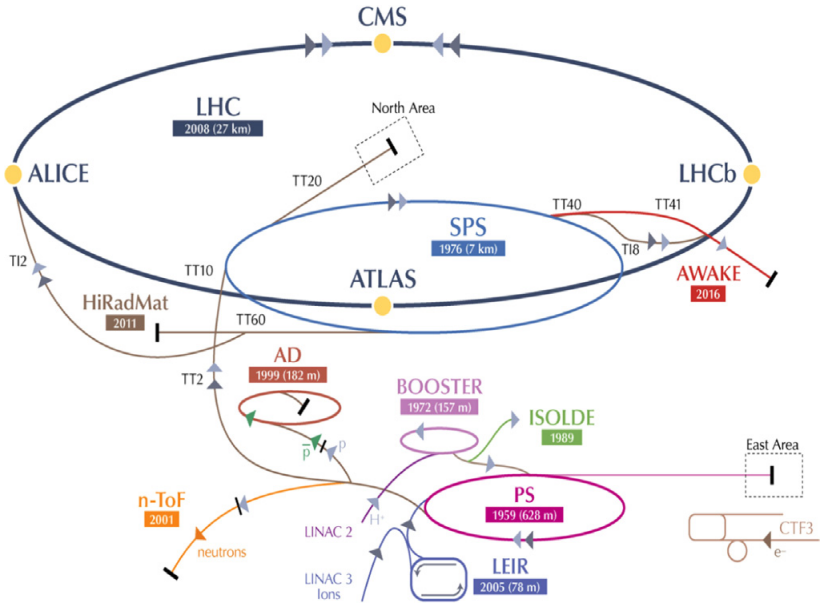

FIG. 1: Map over different accelerators and experiments as CERN, the AWAKE-experiment is to the right in a side tunnel from the SPS (Super Proton Synchrotron). Copyright CERN.

The AWAKE experiment is installed at the same beam line as the former CNGS experiment, as shown in FIG. 1. It uses the SPS-beam with 400 GeV to create plasma wakefields in a 10 meter long plasma cell. The goal is to demonstrate a long acceleration stage without ruining the quality of the accelerated electron beam. The first phase of the experiment, which started in 2016, is to prove that self-modulation instability (SMI) of protons in the plasma will happen as predicted.

In the second phase of the AWAKE experiment, Run 2, the goal is to accelerate a beam of electrons in the proton driven. Two plasma cells are needed for this phase: one to self-modulate the proton beam, and one into which the electron beam to be accelerated will be injected. It is foreseen that we will have a vacuum gap between the two plasma cells, where the electron beam will be injected by steering it parallel to the proton beam. Such a two cell design however, presents a problem since the proton beam will expand radially in vacuum gap. After this vacuum expansion, and the corresponding reduced charge density, the beam may become unusable as a plasma drive, depending on the length of the gap. It is therefore necessary to refocus the proton beam in this gap , before entering the accelerating plasma cell.

Using conventional quadrupole magnets to refocus the beam will require a significant amount of beam line, perhaps more than what is available even upstream. An alternative solution, studied in more detail in this thesis, is to use plasma lenses for the plasma interstage focusing instead.

The concept of using plasma as a lens to focus a particle beam was first discussed in a paper from Berkeley in 1950[8]. It has been used recently for laser-driven plasma wakefield acceleration[9], in a plasma interstage setup similar to that of AWAKE. The plasma lens sizes are on the scale of centimeters, while quadrupole magnets usually are in the meter range. The plasma lens also have another advantage in that it can focus both transversal planes in one stage. In order to focus in both planes, several regular magnetic quadrupoles usually need to coupled together with empty space in between, which further increases the spatial requirements for quadrupoles with respect to plasma lenses.

In this thesis we study so-called active plasma lenses. These consists of gas (could be for example hydrogen, helium or nitrogen) confined inside cylinders. The gas is ionized by an external discharge current, achieved by setting up a voltage of up to 20 kV across the gas cylinder. Such a plasma lens is shown in Fig. 2. A main goal in this work is to evaluate whether plasma lenses can be applied to AWAKE Run 2, i.e. whether we can focus the proton beam in order to inject electron beams while still maintaining the beam quality. As plasma lenses are a new and relatively unstudied technology, a main part of this work is to study the beam-plasma parameters where plasma lenses are expected to cleanly focus a beam.

In this thesis I will first study a key constraints of active plasma lenses: the defocusing effect of wakefields in the lens, competing with the desired linear focusing fields of the discharge current. I do this by implementing a linear plasma wakefield model, and vary parameters (the gas pressure, i.e. the plasma density, and the beam charge and size), to see where the undesired wakes start to have an significant effect. This will be checked against with numerical simulations done with QuickPIC, an open source particle-in-cell code. The results from linear theory will furthermore be tested experimentally at the CLEAR test facility at CERN.

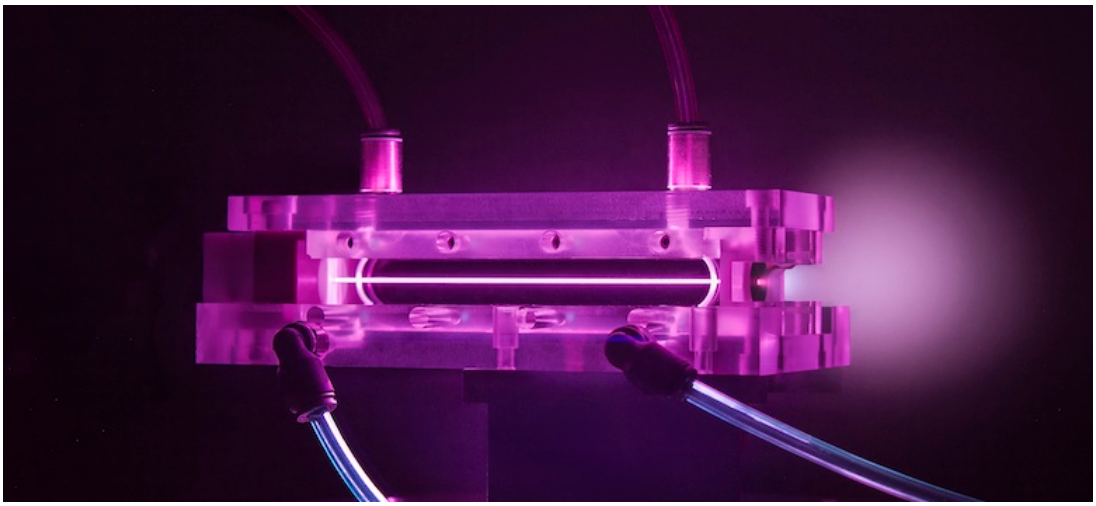

FIG. 2: A picture of a discharge capillary plasma lens, from the Berkely Lab. We see that gas tubes in the bottom, and the high-voltage electrodes at the top. Copyright LBL[10].

The results of the previous analysis will be applied in order to help assess the use of plasma lenses for AWAKE. Is it possible to use a single plasma lens to focus the proton beam between the two cells, so that the wake is mostly unaffected in the entrance to the second plasma cell? Will the the beam quality and degree of self-modulation still be good? We will work with both ideal Gaussian beams as well as realistic proton beams provided by partners from the AWAKE collaboration, after the four meter long plasma.

II. THEORY

A. Beam optics and conventional focusing

To ease some calculations, we shall assume a cylindrical model for the beamline and plasma lens, and use a bivariate gaussian as the theoretical beam. The charge distribution of the beam will in other words be defined as

$$\Psi = \frac{Q}{(2\pi)^{3/2}\,\sigma_\xi \sigma_r^2} \exp\left[\frac{-\left(\xi-\mu_\xi\right)^2}{2\sigma_\xi^2} + \frac{-\left(r-\mu_r\right)^2}{2\sigma_r^2}\right] \tag{1}$$

where ξ is the direction along the beam line, Q the total charge and r the transversal direction. The beam momentum in r has also a Gaussian distribution, with variance $\sigma_{r\prime}^2$.

We are also going to include a distribution of momenta, which can be used to define

$$\beta = \frac{< r^2 >}{\epsilon} \tag{2}$$

$$\alpha = -\frac{< rr' >}{\epsilon} \tag{3}$$

$$\gamma = \frac{1+\alpha^2}{\beta} \tag{4}$$

where r' is the transverse momenta, and ϵ the normalized emittance. α and β are the Twiss parameters[11], and are used for calculation on focusing of a beam. They are connected via the covariance matrix of the transverse position and momentum.

$$\Sigma = \mathrm{cov}\left(r, r'\right) = \epsilon \begin{pmatrix} \beta & -\alpha \\ -\alpha & \gamma \end{pmatrix} \tag{5}$$

To focus a charged beam we usually use magnetic quadrupoles. From multipole expansion for the magnetic field, the first order will be $B_x = -gx$. Here x here is one of the transversal direction, and g the field gradient. The quadrupole strength, normalized to the beam momentum, is defined as

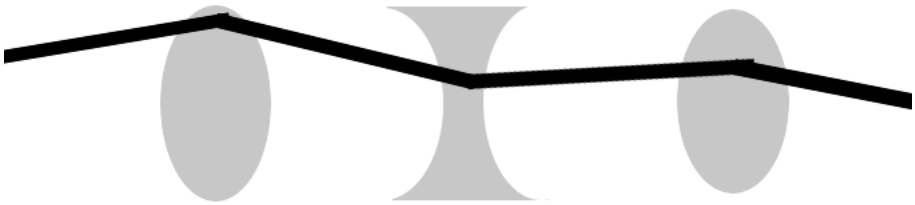

FIG. 3: How a particle with positive transverse position and momenta will evolve through a triplet. Here the first and third magnet are focusing quadrupoles with positive focal length, while the defocusing quadrupole in the middle have a negative focal length.

$$k = \frac{eg}{p} \tag{6}$$

where e is the elementary charge and p the particle momentum. A quadrupole will focus in one transversal direction while defocusing at the same time in the other direction. We need in other words several quadrupoles after each other to get a complete focusing effect, usually in triplets. A sketch of the evolution in a triplet is shown in Fig. 3, where we observe that a divergent beam will become convergent.

Beam optics is defined in the same manner as conventional optics, the focal length for the quadrupoles is $f = 1/kL$, where L is the length of the quadrupole. If the focal length is smaller than the lens width, we can use a thin lens approximation:

$$\mathbf{M}_{\text{Thin}} = \begin{pmatrix} 1 & 0 \\ -1/f & 1 \end{pmatrix} \tag{7}$$

Here $\mathcal{M}$ refer to a transfer matrix of the particle in the phase space[12], which will rotate the particles such that

$$\vec{x}_1 = \mathbf{M}\vec{x}_0 \tag{8}$$

where $\vec{x}$ is the phase space (x, x').

If we want to defocus the beam instead, we substitute $-1/f \to 1/f$. If the focal length is not smaller than the lens width, we use a thick lens approximation. Such a transfer matrix is defined as

$$\mathbf{M}_{\text{Thick}} = \begin{pmatrix} \cos\left(l_p\sqrt{k}\right) & \sin\left(l_p\sqrt{k}\right)/\sqrt{k} \\ -\sqrt{k}\sin\left(l_p\sqrt{k}\right) & \cos\left(l_p\sqrt{k}\right) \end{pmatrix} \tag{9}$$

for a focusing quadrupole, and hyperbolic functions in the defocusing case. Evolution of all beam particles can then be calculated as a transformation through each element of the beam lattice.

$$\vec{x}_1 = \mathbf{M}_Q \odot \mathbf{M}_D \odot \mathbf{M}_Q \odot \mathbf{M}_D \cdots \vec{x}_0 = \mathbf{M}\vec{x}_0 \tag{10}$$

where $\vec{x}$ is the ensemble of particles and $\mathbf{M}_D$ the vacuum drift of length L between the different quadrupoles,

$$\mathbf{M}_D = \begin{pmatrix} 1 & L \\ 0 & 1 \end{pmatrix}. \tag{11}$$

You can similarly do the same with the Twiss parameters for the whole beam, $\mathbf{B}$, with Σ from Eq. 5[12],

$$\mathbf{B} = \Sigma/\epsilon \tag{12}$$

$$\mathbf{B}_1 = \mathbf{M}\mathbf{B}_0\mathbf{M}^T \tag{13}$$

B. Plasma lenses

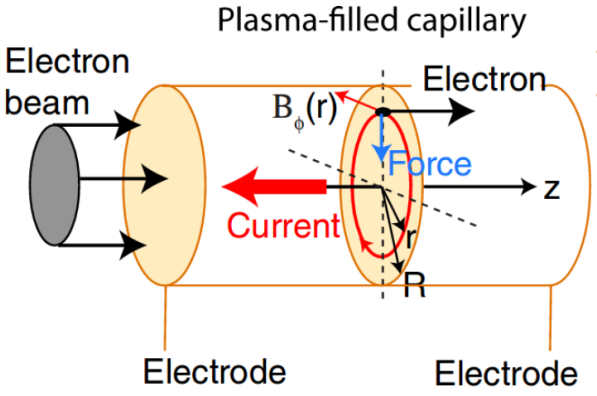

FIG. 4: A sketch of the plasma lens. Electrodes are mounted at the ends of the plasma lens. Applying a high voltage across the electrodes will result in a uniform current in negative longitdunal direction compared to the incoming particle beam. The current create a azimuth magnetic field, which will give a radial force component on the particles in the beam. Copyright Tilleborg[9].

With the framework above for quadrupoles in mind, let's then look at plasma lenses. We start with a cylindrical capillaries in which we inject gas.

Applying a high voltage (order of 10 kV) across the capillary ends the gas will be ionized - a plasma will be created inside the capillary - and a strong discharge current (order of several 100 A) will flow through the capillary. A beam sent into the capillary, propagating parallel to the beam direction will be focused (or defocused) by this current. This focusing device is called an active plasma lens[9]. Such a plasma lens is shown in Fig. 4. Using Amperer′s Law, we find the corresponding azimuth magnetic field

$$\frac{\partial B_\phi}{\partial_r} = \frac{\mu_0 I_0}{2\pi R^2}, \tag{14}$$

where R is the capillary radius of the lens, and I_0 is the current flowing through the lens.

From Eq. 14 we see that if the current is uniform radially inside the capillary, the strength of the magnetic field will increase proportionally to r, just as for a regular mag-

netic quadrupole magnet. In this text we discuss both such ideal, linear plasma lenses and more realistic lenses where the r-dependence of the field is non-linear.

Similarly to Eq. 14 for quadrupoles we express the normalized strength of the plasma lens as

$$\mathrm{k} = \frac{e}{m_0 \gamma c} \frac{\partial B_\phi}{\partial_r}, \tag{15}$$

where e, m_0 are the electron charge and rest mass respectively.

1. Sources of nonlinearities

An ideal plasma lens would have a radially uniform current. Deviations from a radially uniform current, leading to a non-linear focusing force may lead to emittance growth when a beam is focused. It has recently been shown in magneto-hydrodynamics plasma simulations [13] that due to small radial variations in the temperature of the plasma, the conductivity is however not radially independent. The plasma furthest from the center will be cooled down by the lower temperature outside. This is predicted to result in a current flow that is non-uniform radially, and therefore a focusing force that is non-linear. In this text we will use the model of the non-uniformity from [13]

$$J(r)\, \alpha\, T_e(r)^{3/2} \tag{16}$$

to evaluate the effect of non-uniformity of plasma lenses for AWAKE.

Another source of nonlinearities in active plasma lenses is the plasma wakefield set up by the charged particle beam. The longitudinal fields of wakefields are beneficial for accelerating trailing bunches at high gradients[5]. However, the nonlinear transverse fields of such wakefields will be superimposed on the field from the discharge current of the plasma lens. The effect will be studied in some detail in the following section, and the parameter space for when the effects of the wakefields are negligible will be discussed.

C. Linear plasma wakefield theory

We therefore define a linear plasma wakefield model to check if wakes are a significant effect in the plasma lens. As mentioned before, plasma can be seen as a ionized gas and globally neutral. However, due to free electrons, you will have internal oscillations due to electrostatic forces[14]. Such oscillations for electrons are characterized by the plasma (electron) frequency:

$$\omega_p = \sqrt{\frac{n_0 e^2}{\epsilon_0 m_0}} \tag{17}$$

where n_0 is the plasma density, e the elementary charge and m_0 the electron mass. When we send a charged beam through the plasma, it will perturb the electromagnetic fields in the plasma. If the beam has a lower density than the plasma, the wake fields from the beam will be linear. The opposite case is the blow-out regime, where the plasma break down creating charged bubbles, with strong longitudinal electric fields. That regime is used for the plasma wakefield acceleration.

In the linear regime, plasma wakefields can be calculated analytically. We will in the following develop the equations for linear plasma wakefields, and use these to estimate the focusing field contribution from the wakefields in a plasma lens. We will see that for the parameters we are interested in, the fields become significant before the beam density approaches the plasma density. This means that the assumption of the linear regime is a good one. We follow the same procedure as Blumenfeld[15], starting with the continuity equation and the Lorentz force for the electrons in the plasma.

$$\frac{\partial n_e}{\partial t} + \nabla \cdot (n_e \vec{v}_e) = 0 \tag{18}$$

and

$$\frac{d\vec{p}_e}{dt} = -e\left(\vec{E} + \frac{\vec{v}_e \times \vec{B}}{c}\right), \tag{19}$$

where n_e is the plasma electron density, $\vec{v_e}$ the plasma electron density and $\vec{p_e}$ the plasma electron momentum respectively. We then assume that the variation of the plasma density due to the wakes from the beam is much smaller than the plasma density for the whole plasma, n_0. We also assume small velocity and variation, giving

$$n_e = n_0 + \delta n \tag{20}$$

$$\vec{v_e} = v_0 + \delta\vec{v} \tag{21}$$

We insert this into Eq. 18, neglecting second order terms.

$$\frac{\partial \delta n}{\partial t} + n_0 \nabla \cdot (\delta\vec{v}) = 0 \tag{22}$$

Similarly, assuming that the variation of the velocity depend only on time and that electric fields will dominate, for Eq. 19.

$$m\frac{\partial \delta\vec{v}}{\partial t} = -e\vec{E} \tag{23}$$

We can combine them by taking a time derivative of Eq. 22.

$$\frac{\partial^2 \delta n}{\partial t^2} + n_0 \nabla \cdot \frac{\partial}{\partial t}(\delta\vec{v}) = 0 \tag{24}$$

$$\Rightarrow \frac{\partial^2 \delta n}{\partial t^2} - \frac{n_0 e}{m}\nabla \cdot \vec{E} = 0 \tag{25}$$

We calculate the divergence of the electric field by Gauss′ Law, and set the full charge density to be

$$\rho = e\left(n_i - n_e - n_b\right) \tag{26}$$

where n_b is the beam density, and n_i the ion density. Since globally plasma is neutral, this must equal the plasma electron density, $n_i = n_0$. The divergence can then be written as

$$\nabla \cdot \vec{E} = -\frac{e}{\epsilon_0} (\delta n + n_b) \tag{27}$$

Which we insert to 25.

$$\frac{\partial^2 \delta n}{\partial t^2} + \frac{n_0 e^2}{\epsilon_0 m} \delta n = -\frac{n_0 e^2}{\epsilon_0 m} n_b \tag{28}$$

We observe that the terms infront equals the plasma frequency from Eq. 17. Replacing to get

$$\frac{\partial^2 \delta n}{\partial t^2} + \omega_p^2 \delta n = -\omega_p^2 n_b \tag{29}$$

In accelerator physics we usually work a longitudinal coordinates co-moving with the beam, ξ. Transforming the equations using $\xi = z - ct$, we get

$$\frac{\partial^2 \delta n}{\partial \xi^2} + k_p^2 \delta n = -k_p^2 n_b \tag{30}$$

where k_p is the inverse of the plasma skindepth

$$k_p^{-1} = \frac{\omega_p}{c}. \tag{31}$$

We can find an equation for the plasma electron variation with a Green′s function on Eq. 30. We then get finally:

$$\delta n\left(\xi,\vec{r}\right)=-k_p\int_r^\infty n_b\left(\xi',r\right)\cos\left[k_p\left(\xi-\xi'\right)\right]d\xi' \tag{32}$$

We shall use this to find the two-dimensional electric field for linear plasma wakefield. Let us first define the wave equation, with a source term from the electric field in Lorentz gauge:

$$\frac{1}{c^2}\frac{\partial^2\vec{E}}{\partial t^2}-\nabla^2\vec{E}=-\mu_0\frac{\partial\vec{J}}{\partial t}-\nabla\left(\nabla\cdot\vec{E}\right) \tag{33}$$

Where $\vec{J}$ is the current density vector. We insert Eq. 27 and expand:

$$\frac{1}{c^2}\frac{\partial^2\vec{E}}{\partial t^2}-\nabla^2\vec{E}=e\mu_0\frac{\partial\left(n_0\delta\vec{v}+n_bc\hat{\xi}\right)}{\partial t}+\frac{e}{\epsilon_0}\nabla\left(\delta n+n_b\right) \tag{34}$$

We co-cordinate transform again with $\xi=z-ct$, using the definition skindepth from Eq. 31 again.

$$-\nabla_\perp^2\vec{E}=-k_p^2\vec{E}+\frac{e}{\epsilon_0}\left(\nabla\delta n+\nabla_\perp n_b\right) \tag{35}$$

where $\nabla_\perp$ is defined as

$$\nabla_\perp=\nabla-\frac{\partial}{\partial\xi}\hat{z} \tag{36}$$

We do not want to look at the wakefields inside the beam, and remove therefore all terms with the beam density. We end up with two equations for the radial and longitudinal electric field:

$$\left(\nabla_{\perp}^{2} - k_p^2\right) E_z = -\frac{e}{\epsilon_0}\frac{\partial \delta n}{\partial \xi} \tag{37}$$

$$\left(\nabla_{\perp}^{2} - k_p^2\right) E_r = -\frac{e}{\epsilon_0}\frac{\partial \delta n}{\partial r} \tag{38}$$

Writing out the left hand side with r, with two dimensions, we will end up with modified Bessel equations of zeroth and first order respectively. This will in turn give, via Green′s functions, the linear wake fields to be defined as:

$$E_z = 4\pi e \int_0^{\infty} \frac{\partial \delta n}{\partial \xi} K_0\left(k_p r_{>}\right) I_0\left(k_p r_{<}\right) r' dr' \tag{39}$$

$$E_r = -4\pi e \int_0^{\infty} \frac{\partial \delta n}{\partial r} K_1\left(k_p r_{>}\right) I_1\left(k_p r_{<}\right) r' dr' \tag{40}$$

where I_ν, K_ν are the modified Bessel function of first and second kind, and $r_>$ is the greater of r and r' and reversed for $r_<$.

III. WAKEFIELD SIGNIFICANCE IN PLASMA LENSES

When a charged beam enters the plasma lens, the interactions will create a wakefield. While you in theory should have a linear transverse focusing effect due to azimuth magnetic field from the uniform current, the wakes can give a nonlinear contribution. If the nonlinear components are too strong the plasma lens may be unusable for focusing.

In this section we shall calculate the maximal transverse gradient of the wakefield, using two dimensional linear wakefield, as calculated in Section II C. This effect will be quantified, and compared with the focusing from the plasma lens. We define here that the nonlinear component is significant if the maximal transverse gradient from the wakefield is at or above 1% of the plasma lens gradient.

Using the definitions for the wakefields in Eq. 39 and Eq. 40, we can see that the fields will depend on the plasma density n_0, bunch charge Q_e, length σ_z and transverse size σ_r. The result should therefore be linear for the bunch charge, while not the case for the other parameters.

At the CLEAR test facility at CERN[16], the University of Oslo will study plasma lenses to be possibly used in the second phase of AWAKE. Part of the experiments is to check for constraints on active plasma lenses to maintain a good beam quality. Such a constraint could be problem with ionization of the plasma from a large capillary radius, nonlinear current contributions or wakes. We shall here look at the theoretical impact of wakefields in this experiments, to be checked against in reality.

Since this calculation is under a assumption of linear regime, and therefore linear wakefield theory, we will simulate the same situation with a particle-in-cell code to verify the validity of the linear regime calculations.

A. CLEAR test-facility at CERN

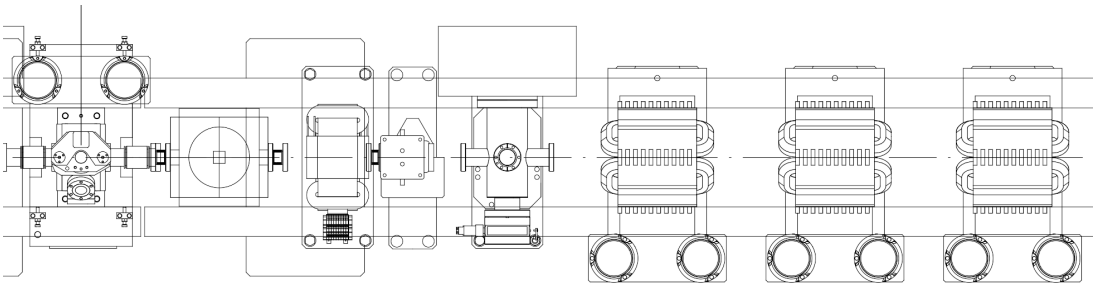

FIG. 5: Current proposal for the CLEAR test facility that will in July 2017 start with experiments with plasma lenses. It has replaced CTF3 (Clic Test Facility 3) at CERN. To the right, outside the figure, the linear accelerator for the electron beam is placed. The beam is finally focused by a triplet of quadrupoles before it is sent through the plasma lens. The plasma lens is the second element from the left. The beam is then measured with a OTR-screen, shown to the far left afterwards. Copyright CERN.

The current proposal for the CLEAR test facility is shown in Fig. 5[16]. The linear accelerator from the CTF3 "main beam" is still kept here, and CLEAR beam will have similar properties. The plasma lens is installed in such a way that we can change it between runs, to a new copy or to a different plasma lens.

Assuming we have room temperature in our experiment, the following parameters in Table I are possible at the CLEAR test facility.

For our simulations we shall keep all of the values of the beam constant, except for the bunch length σ_z and charge Q_e. In the CLEAR experiment we want to study cases where both the effect of the wakefields are estimated to be negligible, and where the effect is significant. For this we study two different beams:

- A short and compressed beam, with a small bunch size
- And a longer beam with a larger bunch size

TABLE I: The CLEAR test facility have the following range of the values the beam can have after the linear accelerator[16]. Shown below are the beam energy, bunch charge, emittance and length; as well as the energy spread. Lower bound for emittance is the lowest bunch charge, and opposite for the upper bound.

Beam parameter	Range of values
Beam Energy E	130- 220 MeV
Bunch charge Q_e	0.01 - 0.5 nC
Normalized emittance ϵ_N	3.0 - 20 mm mrad
Bunch length σ_z	0.5 - 1.2 mm
Relative energy spread ΔE	<0.2% rms (<1 MeV FWHM)

TABLE II: Our assumed values for the gaussian beams used to check for the significance of wakes. They are defined from Table I. We assume a constant beam energy, emittance and beam size, while changing either the bunch charge or length logarithmically.

Simulation parameter	Value
Beam Energy E	200 MeV
Bunch charge Q_e	3.0 - 500 pC
Normalized emittance ϵ_N	3.0 mm mrad
Bunch length σ_z	0.5, 1.5 mm
Bunch size $\sigma_x = \sigma_y$	25, 100 μm

We define a Gaussian beam in cylindrical coordinates, using Eq. 1 and the values given from Table II, to be used in the following. These are ours electron beams in this section. The only significant difference from the realistic values in Table I is the normalized emittance, which we have for this study chosen to be kept constant even for high bunch charge beams.

B. Plasma wakefields in CLEAR

TABLE III: The simulation values for the plasma lens, using parameters from recent papers[17] as a basis The plasma lenses will use nitrogen gas, which gives the domain of pressures. Using Eq. 14, we then found the corresponding uniform gradient in the plasma lens. The azimuth gradient from the wakefield will be compared to this.

Simulation parameter	Value
Peak current I	500 A
Capillary radius R	500 μm
Corresponding lens gradient g	400 T/m
Gas pressure p	0.3 - 30 millibar
Temperature T	300 K

We define an active plasma lens with nitrogen gas, given the values in Table III. Here the current is defined from 20 kV voltage source, which will in turn give a lower bound around a sub-millibar. The temperature is the assumed to be room temperature. The gas pressure and the temperature give us a corresponding plasma density after ionization, using ideal gas law, giving

$$n_0 = \frac{p}{k_b T} \tag{41}$$

Here the pressure p is defined in Pascal, 1 millibar corresponding to 100 Pascal, and k_b the Bolztmann constant. The pressures in Table III will therefore give a plasma density n_0 between 10^{15} to 10^{17} particles/cm^3.

We then did the following: Defined the perturbation of the plasma density due to the wake, $\delta n\,(r, z)$ from Eq. 32, and inserted to the field equations from the wakes in Eq. 39 and Eq. 40. Differentiating the fields gave in turn the gradient of the magnetic field along the radial axis.

The plasma density scale linearly with the pressure, as seen in the definition of the pressure in Eq. 41. This in turn have a linear relation to the density perturbation in

TABLE IV: The upper bounds for the bunch charges, such that the maximal gradient of the wakefield on the longitudinal axis is 1% of the focusing gradient of the plasma lens. If we have a larger bunch charge for a given pressure and bunch length, the effect of the wakefield is then significant and must be taken into account.

Bunch length σ_z \ Pressure p	0.3 millibar	1 millibar	3 millibar	10 millibar
0.5 mm [1% wake]	0.12 pC	0.16 pC	0.23 pC	0.46 pC
1.5 mm [1% wake]	14 pC	31 pC	76 pC	0.23 nC

Eq. 32, so we should see some linearity. The bunch charge Q_e can be shown to be fully linear in comparison. We then calculated for two different bunch lengths σ_z: 0.5 and 1.5 millimeters respectively. For these beam we used a logarithmic increase the pressure p and the bunch charge Q_e, increasing by a factor of $\sqrt{10}$. We will find the domain where the wakefields are significant.

For the short beam we get the maximal transverse gradient on the axis as shown in Fig. 6. Here the transverse gradients are scaling linearly with the bunch charge, while this is not for the different pressures. We can clearly see why this is the case; while we do have a linear factor of the skindepth in the definitions for the wakefields, similarly as for the bunch charge, they are also part of the modified Bessel functions.

In all cases the maximal gradient from the wakefields is larger than 1% of the plasma lens gradient. We must in other words either increase the pressure or decrease the bunch charge. However lower bunch charges will limit the beam diagnostics, at CLEAR the sensitivity is around 1 pC. Increasing the pressure could also lead to gas leakage, which is not optimal when other elements along the beam line have some demands regarding vacuum.

This is however not the case with the longer beam with a much larger bunch size of $\sigma_z = 100\mu$m, and a wider bunch size. From Fig. 7 we can see that more than half of the values will be below 1%. From the second figure you can even find bunch charges that will never give a nonsignificant result for all plasma densities in this domain.

If we assume the result will depend linearly with the bunch charge, we can calculate the upper bound of the bunch charges for which the wakefields should be taken into account. Doing this for 1% of transverse gradient due to the plasma lens current, 4 T/m, we get the result shown in Table IV. We see that for the short beam a 1% constraint is not possible to achieve within our range of values, and we are above 5% even with the highest density and lowest bunch charge. Using the short beam, the wakefields are thus not expected to be negligible.

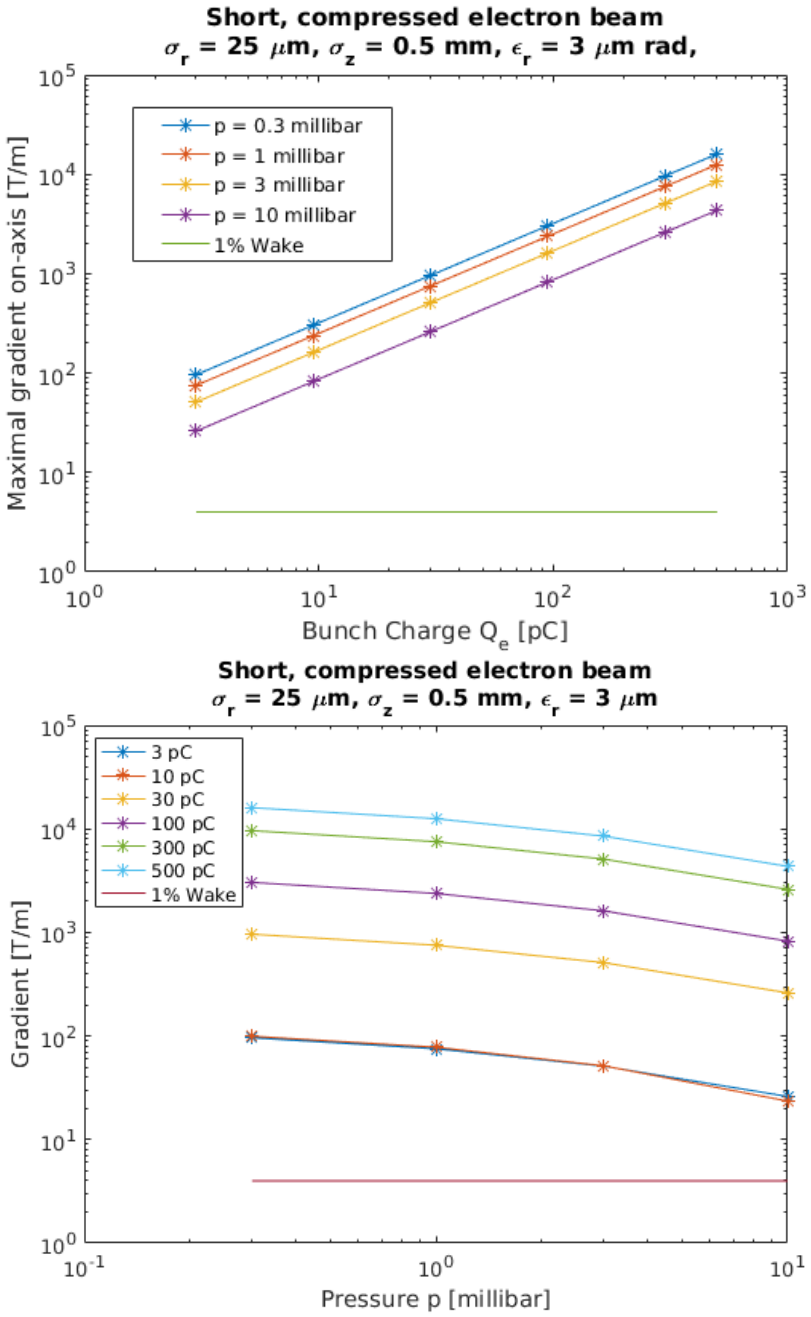

FIG. 6: Plots of the maximal transverse gradient on the longitudinal axis, either when increasing plasma density or pressure, while keeping the other constant. The short beam, with a bunch length of 0.5 millimeters, is assumed here. Also shown in the figures is the line for 1% of axially symmetric focusing gradient, 400 T/m from Table III. We want to find some paramterer space below this line. The pressures are in a decreasing order, higher pressure give a lower line. The opposite is the case for the bunch charges.

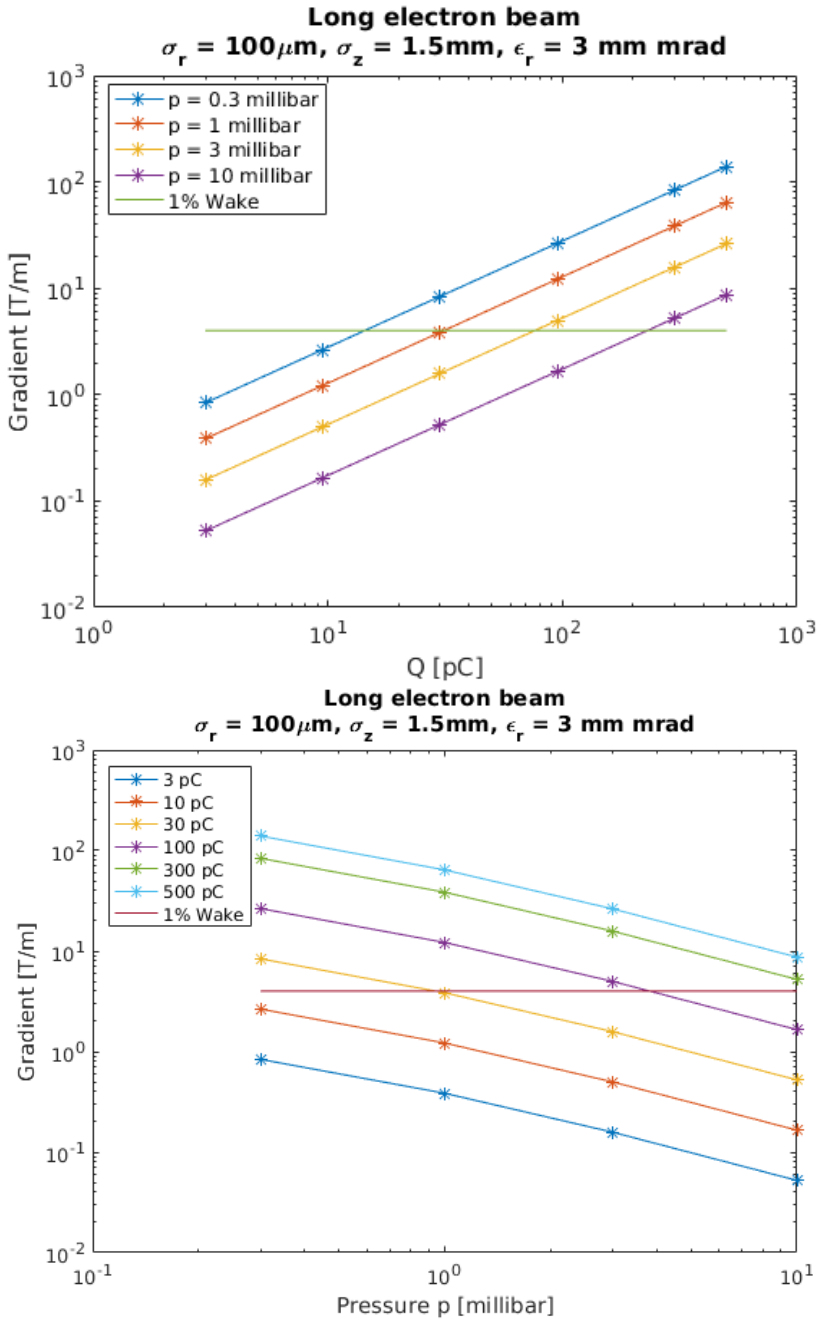

FIG. 7: Maximal transverse gradient for a long beam. Similar to the result in Fig. 6, but here the beam is longer with $\sigma_z = 1.5$ millimeters, and wider. The pressures are in a decreasing order, higher pressure give a lower line. The opposite is yet again the case for the bunch charges. Also shown is the 1%-line of the focusing gradient.

C. Numerical simulation with QuickPIC

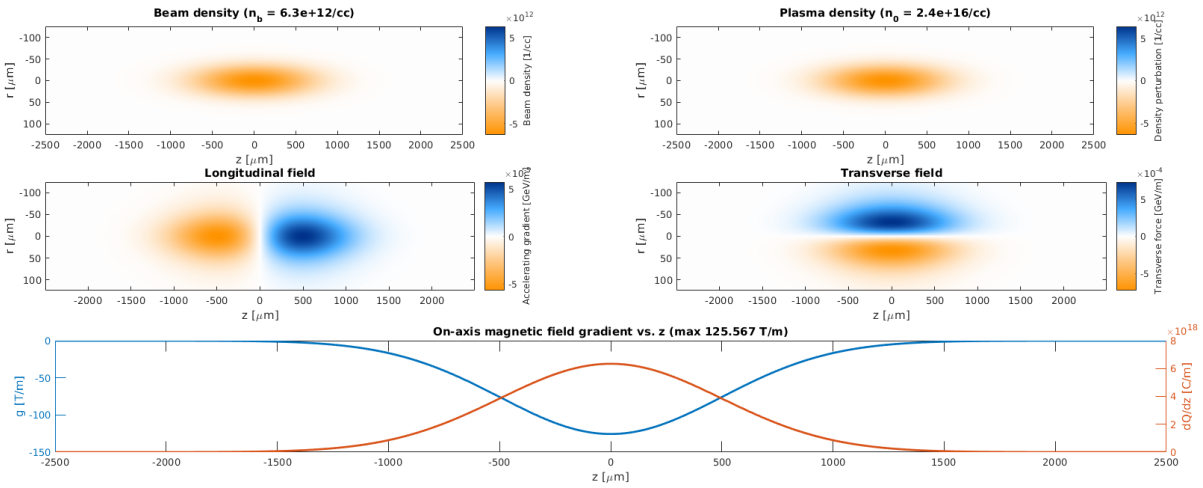

FIG. 8: The result of the calculation of the wakefields using the definitions in Eq. 39 and 40. Shown here are the plot of the beam and plasma density, the fields in both planes and the transverse magnetic field gradient along the z-axis. All are in the XZ-plane, with a maximal field value around 4 GeV/m. We also observe that the gradient has it's maxima in the beam center. We have here assumed a beam with 25μm transverse size, 0.5 millimeters length and a total charge of 5 pC going through plasma, originally from gas with a pressure of 1 millibar

---

Was the linear wakefield theory valid as an assumption? We used QuickPIC, an open-source particle-in-cell code from UCLA[18], to check exactly that. The PIC simulation calculates the dynamics of the plasma electrons, and simulate the interaction with the beam. The simulation assume that the plasma ions are immobile and that we can neglect radiative effects. It is enough to check for a specific case, since the beam density will not change much in our domain of values. We define thus a short beam with

- p = 1 millibar
- Q = 5 pC
- $\sigma_z = 0.5$ mm
- $\sigma_r = 25$ μm,

which gives the fields in Fig. 8. The fields should look like this if the linear wakefield theory is valid. Also in the figure we have the gradient along the longitudinal axis, with a maximal theoretic value of

$$g_{max,\text{theory}} = 125 \text{ T/m} \tag{42}$$

We then simulated a similar radial symmetric Gaussian charged beam with a transverse radius of 25 micrometers, and a bunch length of 0.5 millimeters in QuickPIC. We also used at normalized transverse emittance of 3 microns. The beam is then assumed to travel along z, parallel to the plasma with a plasma density of $n_0 = 2.4 \times 10^{16}$/cm3. Our simulation box here will be [250 μm, 250 μm, 5.0 mm] in x, y, z respectively. The beam is placed in the middle of the simulation box, similar to the beam placement in Fig. 8. We then divide the simulation box in 512 $\times$ 512 $\times$ 4096 cells. This will correspond to a transverse cell width of 0.488 μm, and 1.22 μm in along the beam line.

For QuickPIC the result for the fields, shown in Fig. 10, looks similar to that of the theoretical linear regime, shown in Fig. 8. We also observe that the gradient has the same outline as for the linear regime. We do however have some boundary issues in some of the plots, this is especially the case for the radial gradient. This could not be reduced; we could not increase the resolution or the bunch charge without the simulation breaking apart.

Since we have a even number of cells, the maximal gradient on axis have two values, the maximal gradients of 191 and 140 T/m, giving a mean maximal gradient of

$$g_{max,\text{numerical}} = 167 \text{ T/m} \tag{43}$$

Which is not far away from the theoretical value from the linear wakefield theory for the linear regime. If we were to increase the resolution without problems, the difference would probably decrease.

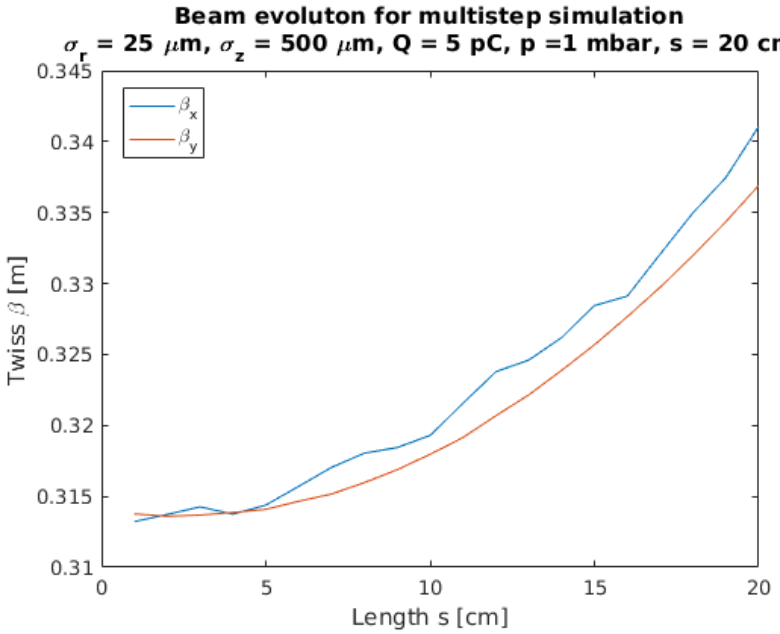

FIG. 9: Evolution of the beam with several steps in QuickPIC. We have here used a time scale that corresponds to the maximal length we shall use for plasma lenses in later sections. Shown are both β_x and β_y as a function of s, where β_x is the uppermost.

We also performed a time-evolved simulation of the system, calculating the forces in each cell and let them interact on the system for 20 centimeters (many time steps), to verify whether the beam density remains relatively inside the plasma cell. The evolution of the Twiss-parameters in this multistep simulation is shown in Fig. 9. How do this increase compare to for example drift in vacuum over the same distance? In vacuum the increase can be expressed as[12]

$$\beta(s) = \beta_0 \left[1 + \left(\frac{s}{\beta_0}\right)^2\right] \tag{44}$$

Which for this case gives that a initial beta of β_0= 0.31 meters will increase to 0.44 meters. This is clearly not the case here, and neither the opposite: that the beam will implode inwards. This implies that the usage of a single wakefield calculation for the whole plasma cell is good enough.

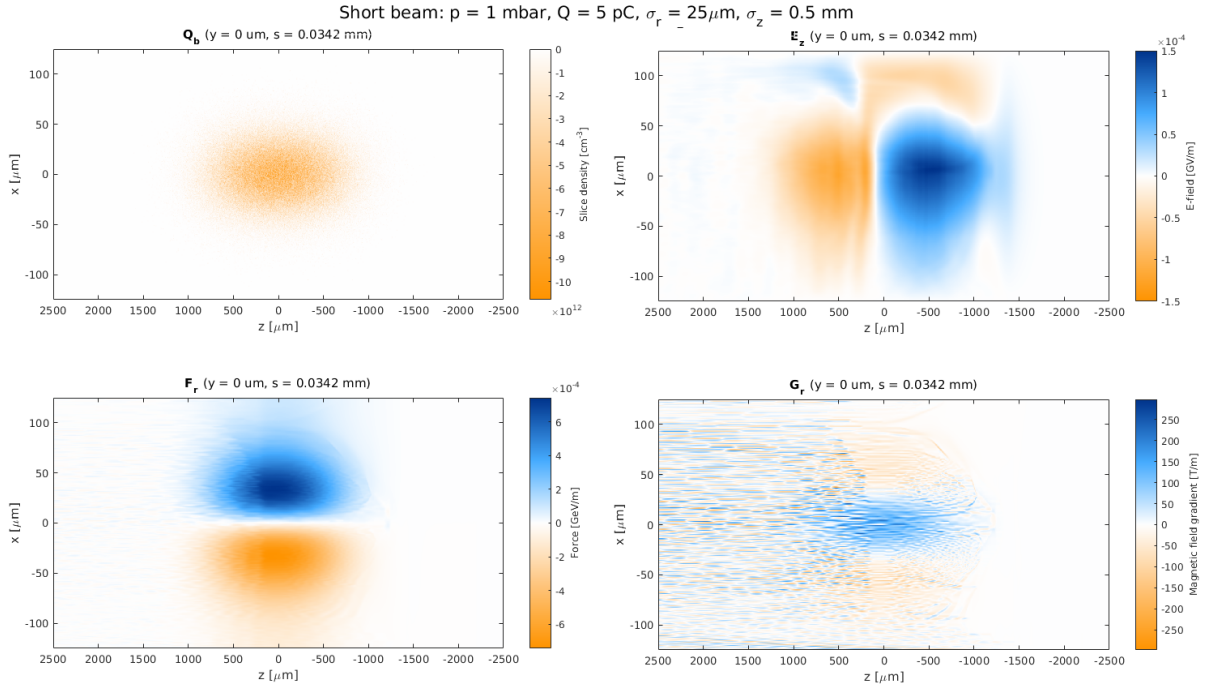

FIG. 10: The same situation as in Fig. 8, but from a simulation with QuickPIC. Shown here are the beam density, the longitudinal and transverse fields and the field gradient, all in the XZ-plane. We also observe here that we have 4 GeV/m for the transverse field, while the longitudinal field seems to be reduced. This is similar to the field values in the theoretical linear regime. All figures also have numerical noise, especially for in the figure for the field gradient, along the edges. Since this does not seem to affect the beam core itself to much, we have not looked further into it.

IV. THE AWAKE PLASMA INTERSTAGE

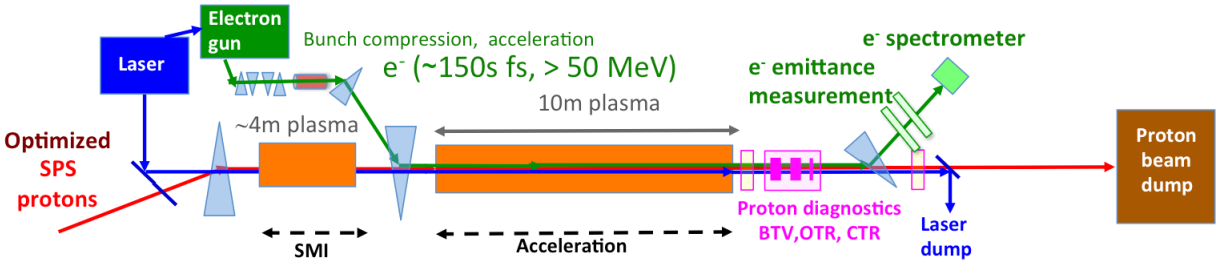

FIG. 11: Current design for the second run of the AWAKE-experiment[19]. To the left the SPS proton-beam is injected to a four meter long plasma cell. This plasma cell will self-modulate the proton beam such that it is bunched in units of the plasma wavelength λ_p. After this process we have a beam pipe where we will focus the proton beam again, while injecting the electron beam at the end. Finally, we have a 10 meter long plasma cell, where the proton beam will be a driver for plasma wakefield acceleration. The focus here will be the portion between the two plasma cells, denoted as the interstage.

One of the main goal of AWAKE Run 2 is to inject and accelerate an electron witness beam.[19][20]. In order to inject an electron witness bunch while preserving its beam quality the proton beam must have fully self-modulated so that wakefield phase and amplitude are quasi-stable in time[21][22]. Two separate plasma cells are therefore foreseen for Run 2, the first cell will modulate the proton beam, while the electron beam will be injected between the first and the second cell.

A sketch of the Run 2 layout is depicted in Figure 11. A main challenge with this approach is to preserve the characteristics of the proton beam in the vacuum gap between the two plasma cells[19]. Simulations show that if the proton beam is propagating more than a few tens of cm in vacuum without refocusing, it may not drive a strong enough wake in the second cell. In this chapter we study the problem of staging the two plasma cells, and in particular whether plasma lenses can be used to provide an interstage design fulfilling the AWAKE requirements.

In the beamline currently used for AWAKE, the maximum distance available for the interstage will be around the order of ten meters. We will have problems expanding further both up- and downstream. Is it therefore possible to use a focusing lattice with

plasma lenses in the plasma interstage, while also leaving enough room for an injection of electron beam right before the final plasma cell? We shall compare the result to regular quadrupoles, as well as include the nonlinearity of the magnetic field due to non-uniform current density in the plasma lenses.

A. The proton beam after extraction

As shown in Fig. 11, the SPS proton beam, which has a mean energy of 400 GeV and a full bunch length of $\sigma_z = 12$ centimeters (2 ns)[20], will traverse about 4 m of plasma in order to self-modulate. Four meter is an estimate of the length required for the self-modulation instability to saturate and the micro-bunching of the beam to fully develop. As input for our AWAKE interstage studies we use a simulated beam distribution where SPS beam has passed through 4 m of plasma, simulated with the particle-in-cell code LCODE[23]. The LCODE simulation output has been kindly provided by Alexey Petrenko (CERN, the AWAKE project). The resulting proton beam transverse and longitudinal phase space is then shown in Fig. 13

However, the only parts of the beams that we need are particles that are within a skin depth in the transversal plane, as only these protons will contribute to the creation of the wakefields in the plasma cell. We therefore apply a transverse cut of the beam, using only one of the transversal planes from here, x from the simulation. The plasma density for the AWAKE plasma cells[20] is

$$n_0 = 7 \times 10^{14} \text{ particles/cm}^3, \tag{45}$$

which, if we apply to Eq. 31 gives a plasma skindepth of

$$k_p^{-1} = 201 \ \mu\text{m}. \tag{46}$$

The new result for phase space and longitudinal distribution are then shown in Fig. 14. Most of the beam here is within 0.2 millirads. We can calculate the initial geometric

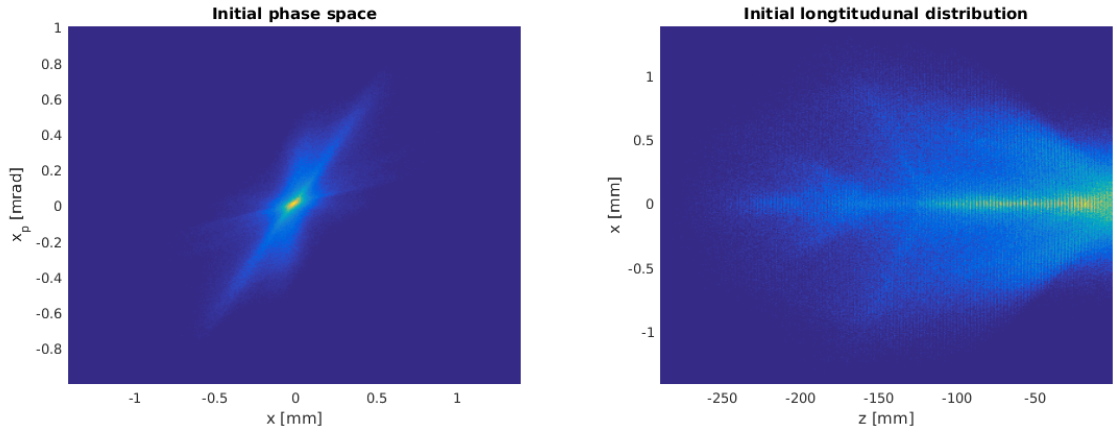

FIG. 12: Simulation data for the SPS-beam after 4 meters of plasma, i.e. after the beam has been self-modulated. Data kindly provided by Alexey Petrenko (CERN, the AWAKE project). To the left we have the initial phase space in the transverse plane x, and to the right the longitudinal distribution along the same plane. We see evidence of SMI by the lines in the longitudinal distribution, and observe that the rear part of the beam is destroyed as well. Only half of the beam is included here, the part that will be self-modulated.

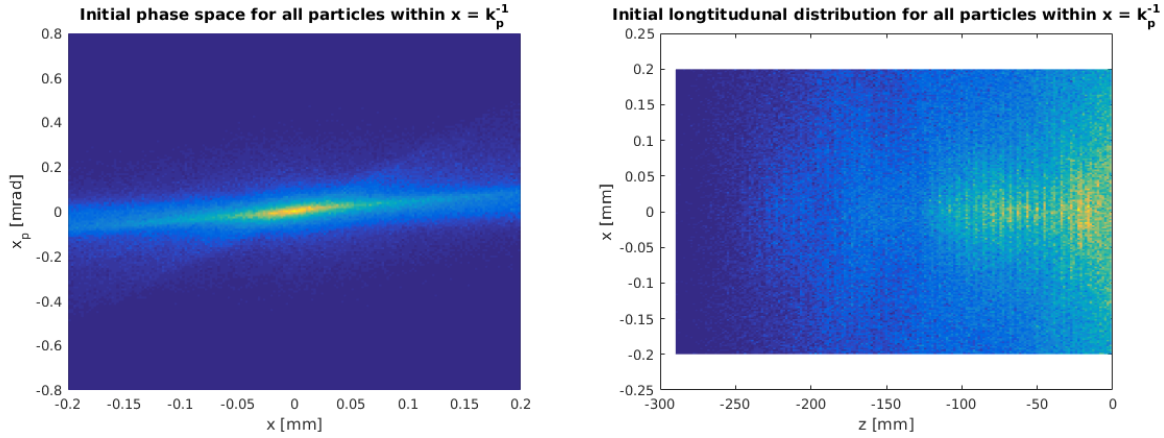

FIG. 13: Same beam as in Fig. 13, where we have removed all particles outside $|x| = k_p^{-1}$. This corresponds to 43% of all the original particles. We see that the particles with high transverse momenta are removed as a result.

---

emittance, standard deviation along x and the Twiss parameters for it as well. This shall be the initial beam properties we will refer to later, and which we want to get back to at the end of the interstage. Using the definitions from Eq. 2 to Eq. 5, we have then the following initial values:

$$\sigma_{x,0} = 104\ \mu\text{m} \tag{47}$$

$$\epsilon_{x,0} = 0.0149\ \text{mm mrad} \tag{48}$$

$$\alpha_{x,0} = 0.321\ \text{m} \tag{49}$$

$$\beta_{x,0} = 0.726\ \text{m} \tag{50}$$

Another aspect we should look at after refocusing the beam is what amount of the beam is still self-modulated. This is crucial to keep if we want to use the proton beam as a driver beam for the next plasma cell. If we fourier transform the longitudinal distribution for both the full and plasma skindepth-cut beam, we can see which wavelengths are dominating. The result is shown in Fig. 12, where we can see a peak at exactly the plasma wavelength, $\lambda_p = 1.26$ millimeters, with a corresponding amplitude:

$$A_0 = 43.2 \tag{51}$$

For the final beam we then fourier transform and study the change of the amplitude for same peak. We denote the amount of protons still self-modulated as N,

$$N = A_{final}/A_0 \tag{52}$$

where A_final is the amplitude for the final beam.

1. Wake significance for the AWAKE interstage

The proton beam from SPS could possible be ruined by wakefields in the plasma lenses, as was discussed in previous Section III A for the CLEAR pre-study. Using linear plasma

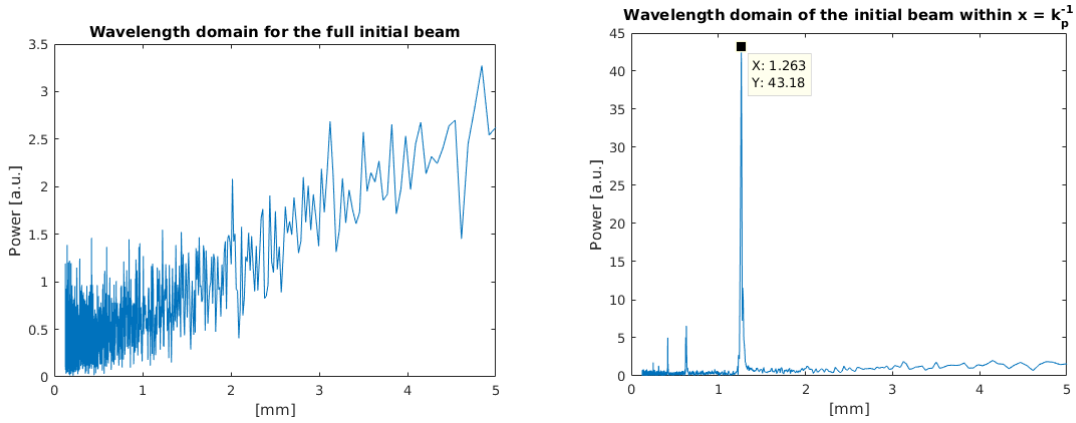

FIG. 14: The fourier transform of the initial particle distribution along the beam pipe, where we should see a peak for the plasma wavelength as an indication of self-modulation. We clearly can see such a peak if we only include particles within one plasma skindepth, in the figure to the right. We denote the value of the peak as $N = 100\%$ of the initial self-modulation.

---

wakefield theory for the full beam, as defined in Table 1 from Gschwendtner[20] , we then have as a maximal destructive gradient:

$$g_{\max} = 6.30 \text{ T/m} \tag{53}$$

where we have also assumed a plasma density of 10^{17} particles/cm^3 (10 millibars) for the plasma lenses. We assume we still are above the linear domain, and the result is valid. The nonlinearity due to wakefields are therefore nonsignificant for plasma lens with a radius of 0.5 millimeters; this will be within 1% if we use a current of 1 kA. If we then increase the radius to 1 millimeter, the gradient due to the wakefield will have increased to 3% of the focusing gradient, and up to 7% if we have 1.5 millimeters instead. We should therefore try to limit most the plasma lenses to within 1 millimeter.

B. Interstage lattice designs

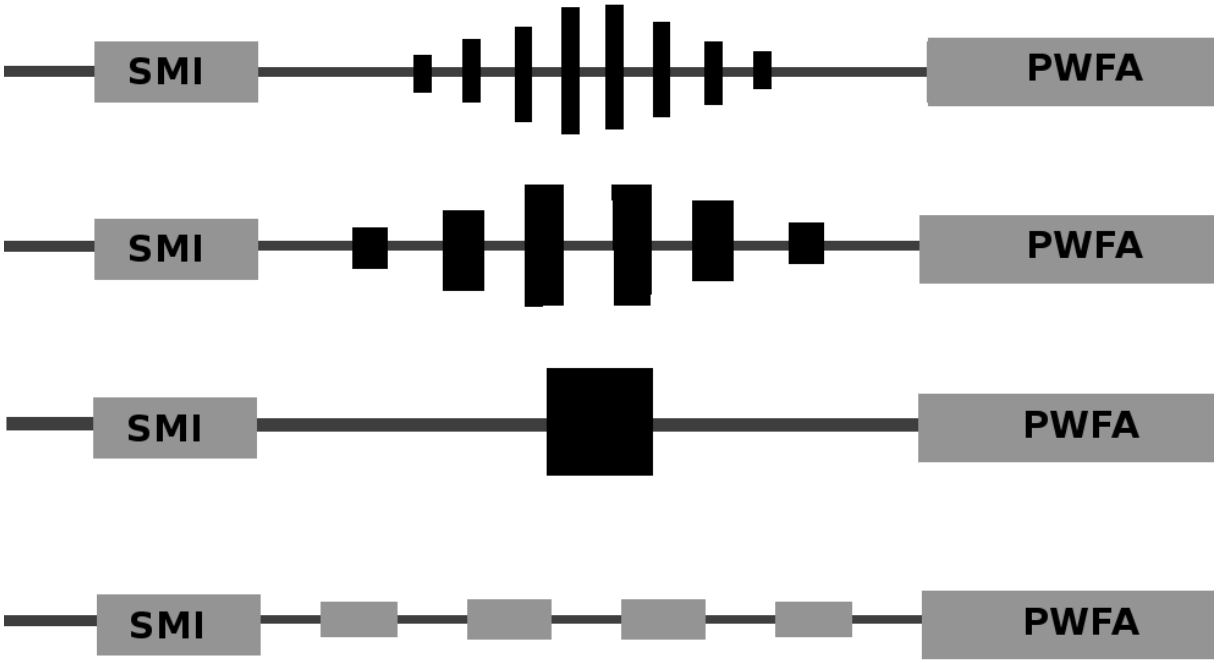

FIG. 15: We shall here look at four different case: 1) plasma lenses of today, with 1 meter of initial gap; 2) a case with longer plasma lenses and less initial gap, 3) a single long high current plasma lens, and finally 4) a line of focusing quadrupoles instead. The beam is here going from the left, and the amount of elements in each lattice are arbitrary.

With the proton beam in mind, we start looking at different options to focus the proton beam in the interstage. If we have around one meters of gap the last lattice element, we will have enough space in the beam line to insert a dipole, for injection of the electron beam. To get symmetric designs we then also define the gap to the first element to be the same. This shall be a constraint for most of the designs. Currently we have two possible options to refocus the beam:

- Axisymmetric plasma lens focusing
- Conventional quadrupole focusing

For plasma lenses we shall look at three different possible design: an initial design, with current available technology; a possible shorter design in the future, with better

plasma lenses, and a single high current plasma lens instead. The nominal current is set to 1 kiloampere, which is the upper bound of what is achievable today. Finally we shall use conventional quadrupoles to see if the distance will be significant shorter. Here we only focus in one plane, to get a lower boundary estimate. The lattice designs will look like the ones sketched in Fig. 15, where the number of lenses for the plasma lenses are arbitrary.

In order to compare the different interstage designs, we shall calculate:

- The fraction of core particles surviving the interstage transport
- The Twiss parameters, α and β, for the final beam after the transport. These are defined in Eq. 3 and Eq. 2 respectively, and define the transverse characteristics of the beam. The more they change after the transport, the more the proton beam will be away from equilibrium with the plasma[24].
- The degree of self-modulation remaining after the transport, N, which depends on the longitudinal distribution of the core of the beam.

1. Initial plasma lens design

Recent papers from Berkley[13] imply that a lens of the order of ten centimeters and half a millimeter radius is available as of today. A longer plasma cell will have problem with ionization, while a larger plasma lens radius will just reduce the plasma lens gradient. The distance between each plasma cell must also be larger than the length of plasma lenses themselves. The initial parameters for the first design are therefore defined as the following:

$$L_0 = 1.0 \text{ m} \tag{54}$$

$$L_{\text{gap}} = 0.2 \text{ m} \tag{55}$$

$$l_p = 0.1 \text{ m} \tag{56}$$

$$I_p = 1.0 \text{ kA}, \tag{57}$$

where L_o denote the gap between the plasma lens lattice and the two plasma cells, L_{gap} the distance between the plasma lenses, l_p the length of the lens and I_p the current in each plasma lens.

The following was then done to achieve symmetric matching of the Twiss parameters in the interstage. We calculated the covariance matrix for the beam in the x-plane before each plasma lens, and updated the current beam properties. We then defined the new plasma lens with a radius such that 3 standard deviations of the beam survives, i.e.

$$R_p = 3\sigma_{x,\text{left}} \tag{58}$$

All particles outside this range was removed, and the beam transported to the next plasma lens. When the sign of α_x flipped for the particles left, the radius of the last lens calculated was adjusted such that $|\alpha_x| < 10^{-5}$ halfway to the next plasma lens. We then repeated the same plasma lenses in reverse, such that we have a symmetric point in the middle between the two lenses here. We could have achieved similar result with symmetry point in the middle of a plasma lens instead, which will only shorten the result with one lens.

If we do not change any of the initial values above, we get perfect alpha-matching when we use 58 plasma lenses, resulting in total beam line of 19.2 meters. While the first plasma lens is of the same size as current plasma lenses, the plasma lens radius in the middle is thrice the size. This plasma lens radius will however cut the beam in the middle, since it is smaller than its neighbours. We fixed the problem by increasing the current up by 12%, i.e. $I_p = 1.01$ kA, such that the radius follow the same contour. The resulting beam evolution and the plasma lens radius as a function of the interstage position s are then shown in Fig. 16. The new design will keep 94.2% of the initial cut beam. We observe that the maximal envelope at the middle for β is 28.7 meters as well.

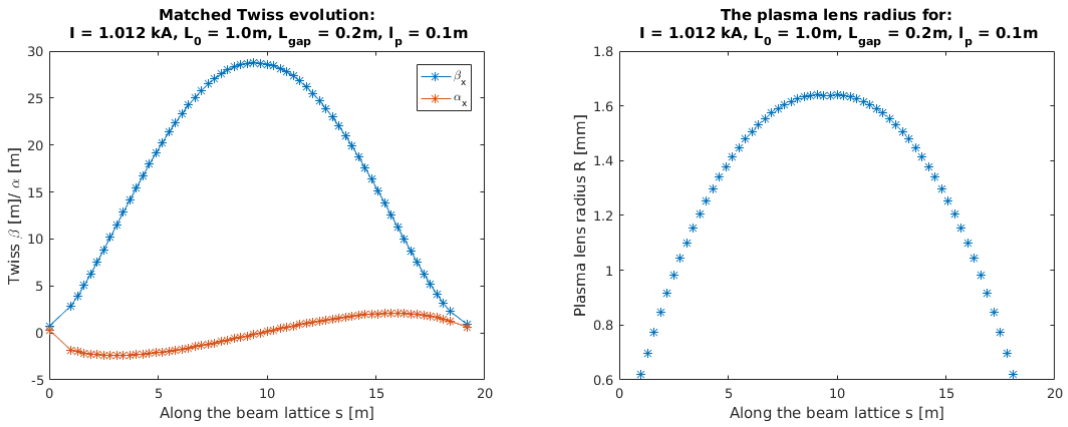

FIG. 16: The resulting beam line, if we do not change any of the initial parameters, will demand a beam lattice of 58 plasma lenses. Shown here are the evolution of the Twiss-parameters in meters through such a lattice, to the left, and radius of each plasma lens in millimeters to the right. β is the line most uppermost. The method of only tweaking the lens in the middle result in a smaller radius here, which will cut away parts of the beam. Changing the current by a little for all plasma lenses will increase the radius of the middle lenses such that no particles will be unnecessary cut.

For this configuration, with an initial drift of 1 meters, lens distance of 20 centimeters and a lens length of 10 centimeter, we then find the acceptance map. This is a parameters scan of all possible transverse position and momenta a particle can have, and survive the lattice. The result is shown in Fig. 17, where the surviving particles are in the middle. We observe a boundary that is the same around a symmetry axis along the diagonal.

We should also look at the final beam, to see if it still looks good. The corresponding phase space and longitudinal distribution are shown in Fig. 18, where we have used the same limits as the initial beam. The beam has collapsed along the middle the beam, while this effect is less clear in the front. The phase space also seems to be the same for small transverse momenta and in the beam center, while all particles with high transverse momenta has again died. For the final beam we have then, using the definitions in Eq. 3, 2, 52;

$$\sigma_{x,\mathrm{ID}} = 115\ \mu\mathrm{m} \tag{59}$$

$$\epsilon_{x,\mathrm{ID}} = 0.0149\ \mathrm{mm\ mrad} \tag{60}$$

$$\alpha_{x,\mathrm{D}} = 0.645\ \mathrm{m} \tag{61}$$

$$\beta_{x,\mathrm{ID}} = 0.895\ \mathrm{m} \tag{62}$$

$$N_{\mathrm{ID}} = 100\,\% \tag{63}$$

2. Shorter design with future technology

Ideally we want to achieve a beam lattice design that has a total length of ten meters, a factor two in reduction of the length from the initial design. The number of lenses should also be decreased to a more reasonable amount. Can this be achieved by either decreasing the end lengths, or increasing the plasma lens length and the current used in each plasma lens to a future possible value?

The parameters were changed by a factor two for both the two first cases. When increasing the length of the plasma lens, the gap length was similarly increased. The shorter initial gap is possible today as well, but to the authors knowledge less than 1 meter of gap to the injection of the electron beam will be difficult. A plasma lens of 20 centimeters with uniform field could also be possible in the future. We then have the new parameters defined as:

$$L_0^* = 0.5\ \mathrm{m} \tag{64}$$

$$l_p^* = 0.2\ \mathrm{m} \tag{65}$$

$$L_{gap}^* = 0.3\ \mathrm{m} \tag{66}$$

If we just decrease the initial gap, L_0^*, keeping the parameters defined in Eq. 55 to 57, we can decrease the total length of 30% to 13.4 meters. Such a beam line will keep 93.8% of the initial particles and end up using 42 plasma lenses of 10 centimeters. Similarly if we change the plasma lens length and the gap between them, l_p^* and L_{gap}^* respectively, we then decrease the total length with 28.7% to 13.7 meters. Such a beam will

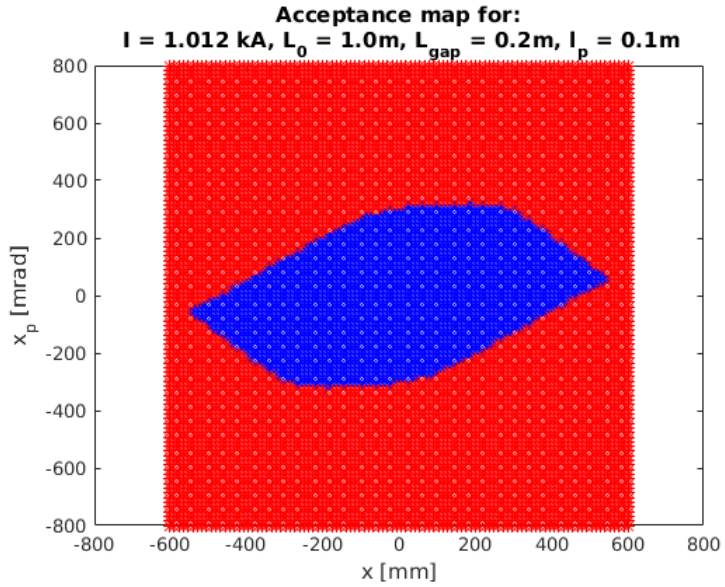

FIG. 17: The acceptance map for initial design, as defined in Eq. 54 to Eq. 57, where the sketched part is the parameter configurations that will survive the lattice. We observe that the longest transverse position is around 550 millimeters, while the highest transverse momenta is around 330 millirad.

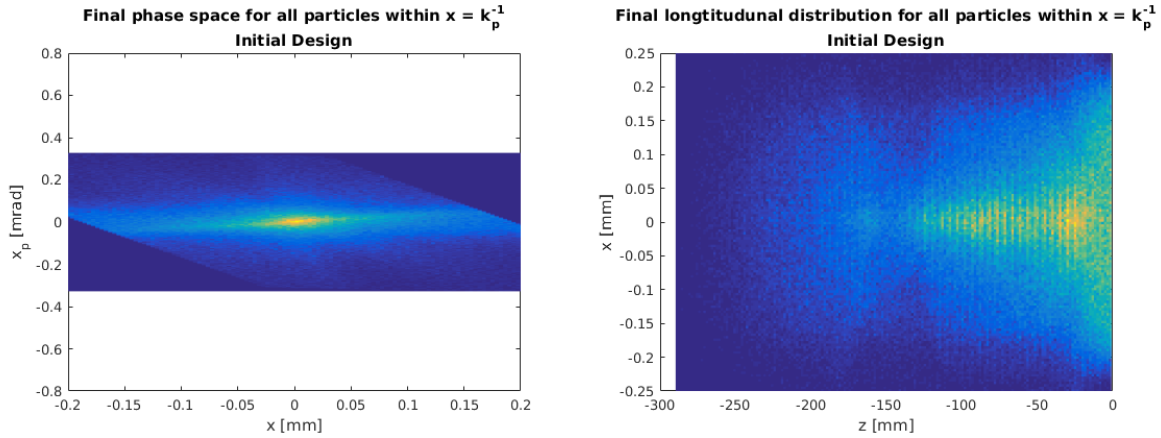

FIG. 18: The final beam after the initial design, as defined in Eq. 54 to Eq. 57, with 19.2 meters of beam line. On the left the phase space is plotted, while on the left we see the final longitudinal distribution. The axes are fixed to the same values of millimeters and millirad as the initial beam, shown in Fig. 14.

---

also keep 94.3% of the initial particles, but will only need 24 plasma lenses compared to 42.

If we combine both of these changes, we should achieve what we want: a reduction by a factor of two in total length while reducing the number of plasma lenses needed. This seems to be the case, the total length end up at 10.7 meters, a reduction of 55.7%. We will similarly keep 94.0% of the beam and the number of plasma lenses reduced to measly 20.

The evolution of the Twiss parameters through the beam line, when we use the shorter design, are shown in Fig. 19 together with all plasma lens radius. We see that the beam does not diverge as much as in the first case before it is focused; β is at it's most 10 meters compared to 29 meters for the initial design. The plasma lens radiuses will also sink as a result, becoming less than 1 millimeters. We can therefore neglect wake-field contributions for this design. The phase space and longitudinal distribution of the beam are indistinguishable to that of the beam from the initial design, as shown in Fig. 18.

The acceptance map for the final beam in this case are shown in Fig. 20. While the maximal transverse momenta is still around 330 millirads, the maximal transverse position to survive the beam as decreased to 400 millimeters, from 550 millimeters in the initial design. We can also for this final improved lattice, denoted as Short Design from here, calculate the final beam properties and the preservation of the self-modulation.

$$\sigma_{x,\mathrm{SD}} = 111\ \mu\mathrm{m} \tag{67}$$

$$\epsilon_{x,\mathrm{SD}} = 0.0149\ \mathrm{mm\ mrad} \tag{68}$$

$$\alpha_{x,\mathrm{SD}} = 0.558\ \mathrm{m} \tag{69}$$

$$\beta_{x,\mathrm{SD}} = 0.824\ \mathrm{m} \tag{70}$$

$$N_{\mathrm{SD}} = 100\ \% \tag{71}$$

All the result for all the four different configurations are finally compiled in Table V. All the maximal plasma lens radii are here larger than the plasma lens radius used to the author knowledge[13], as much as thrice the radius for the initial design. The current is also double of the same lenses used.

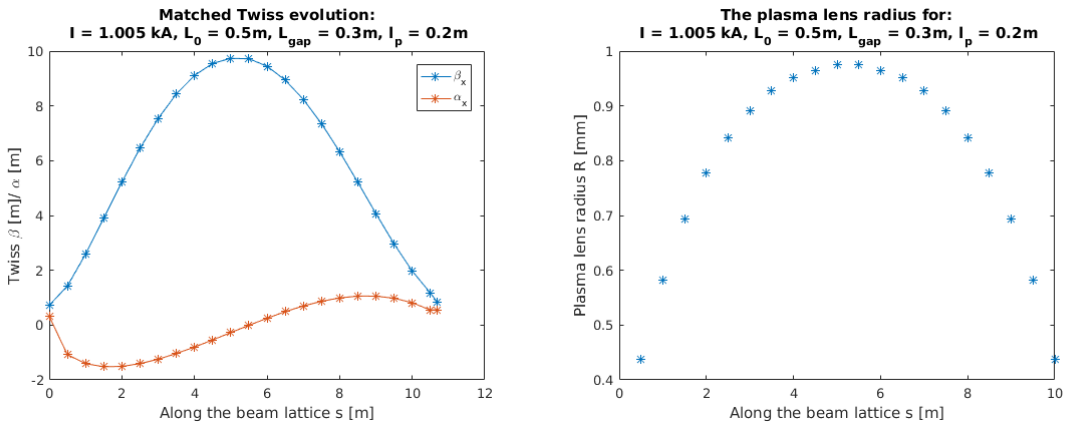

FIG. 19: The matched Twiss evolution with a shorter design, where the current has been tweaked such that the middle plasma lens radius, shown to the left, follows the implied curve. We see that the highest value of the β is at 10 meters , compared to 29 meters in Fig. 16. The largest plasma lens radius is also around 1 millimeters in this design.

TABLE V: All the configurations for the AWAKE interstage with multiple plasma lenses. We look at the current I_p used in all the plasma lenses for that configuration, maximal radius R_p of a plasma lens needed, and the total number of lenses M and the corresponding full length s. We also include how much of the initial cut beam will survive the lattice, as well as the relative difference of α and β from the initial beam cut.

Configuration	I_p [A]	max R_p [mm]	M	s [m]	Survival	Rel. diff. β	Rel. diff. α
Initial design	1.01 kA	1.64 mm	58	19.2 m	94.0%	23.3%	101%
Change to L_0^*	1.05 kA	1.15 mm	42	13.4 m	93.8%	15.4%	82.3%
Change to L_{gap}^* & l_p^*	1.06 kA	1.30 mm	24	13.7 m	94.3%	24.7%	98.7%
Short design	1.01 kA	0.976 mm	20	10.7 m	94.0%	13.6%	73.7%

The possibility of a nonlinear effect should therefore be looked at. All of the designs have also a high relative difference of α_x to the initial α_x from the skindepth-cut beam, this could be a consequence of some of the beam not surviving the lattice. The beam emittance is however conserved in all cases, as well as the degree of self-modulation are in all cases 100%.

3. Single high current plasma lens

What if we used a plasma lens with an increased lens length of say $l_{p,\mathrm{SL}} = 0.5$ meters, with a radius of $R_p = 3\sigma_x$ of the skin depth cut beam after one meter. This will give a plasma lens radius of $R_{p,\mathrm{SL}} = 0.622$ millimeters. Which current is needed to only need one such plasma lens? We want in other words to find a transfer matrix $\mathcal{M}$ such that:

$$\mathcal{M}\begin{pmatrix} x \\ x' \end{pmatrix} = \begin{pmatrix} x \\ -x' \end{pmatrix} \tag{72}$$

Where we assumed that the transversal position x is so small that we can just assume a flip in the angle similar to light rays, i.e. from divergent to convergent momenta. Let us first assume we can use a thin lens approximation, using the matrices as defined in Eq. 11 and 7 to get the total transfer matrix $\mathcal{M}$.

$$\mathcal{M} = \begin{pmatrix} 1 & 1 \\ 0 & 1 \end{pmatrix}\begin{pmatrix} 1 & 0 \\ -1/f & 1 \end{pmatrix}\begin{pmatrix} 1 & 1 \\ 0 & 1 \end{pmatrix} \tag{73}$$

$$= \begin{pmatrix} 1-1/f & 2-1/f \\ -1/f & 1-1/f \end{pmatrix} \tag{74}$$

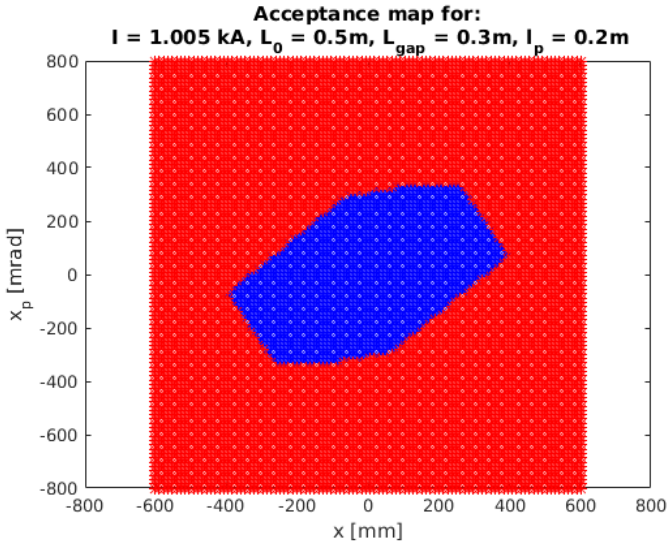

FIG. 20: The acceptance map for short design, where the sketched part is the parameter configurations that will survive the lattice. This figure is to be compared to the acceptance map of the initial design, in Fig. 17.

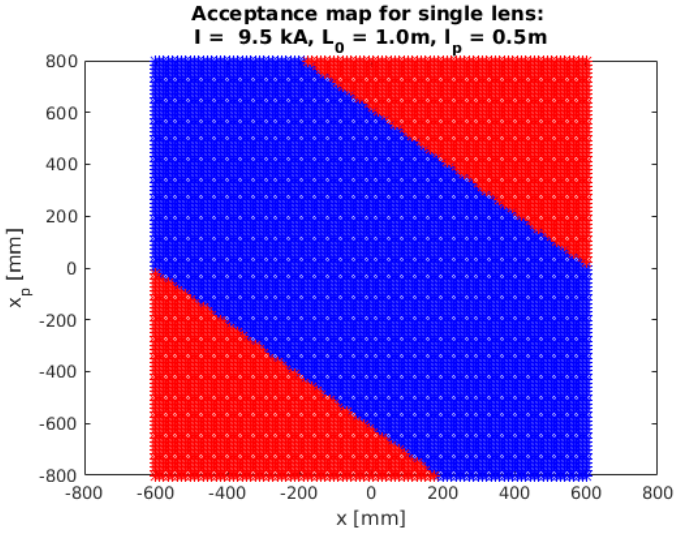

FIG. 21: The acceptance map for the single lens design, where the sketched part is the parameter configurations that will survive the lattice. This figure should be compared to the acceptance maps for the multiple lens configurations, as shown in Fig. 17 and Fig. 20. We see that while the other configurations had a maximal limit on the transverse position and momentum; for a single lens we only need a transverse momenta such that the particle will be within $|x| < 0.621$ millimeters right before the lens, since the momenta will just be swapped.

We can achieve $-x'$ by looking at the bottom line, setting $x << x'$:

$$\begin{aligned}(1 - 1/f)\, x' &= -x' \\ \rightarrow f &= 0.5 \text{ m}\end{aligned} \tag{75}$$

We get a focal length of half a meter. However thin lens approximation is only valid if the focal length is much longer than the plasma length, this is clearly not the case here. Let us however still solve the theoretical result for the thin lens for the initial beam, inserting into beam matrix from Eq. 13 and the focal length from Eq. 75,

$$\mathcal{M} = \begin{pmatrix} -1 & 0 \\ -2 & -1 \end{pmatrix} \tag{76}$$

$$\vec{B}_1 = \mathcal{M} \begin{pmatrix} \beta & -\alpha \\ -\alpha & (1+\alpha^2)/\beta \end{pmatrix} \mathcal{M}^T \tag{77}$$

$$\vec{B}_1 = \begin{pmatrix} \beta & 2\beta - \alpha \\ 2\beta - \alpha & 4\alpha - 4\beta + (1+\alpha^2)/\beta \end{pmatrix} \tag{78}$$

We see from Eq. 78 that β will be conserved, while α will only be conserved in value, but shifted, if β is much less than α In other words our assumption that $x << x'$. For the initial beam this not true; β is larger than α. The core should still be valid, which we check with the full focusing matrix instead, using thick lenses from Eq. 9.

$$\mathcal{M} = \begin{pmatrix} 1 & 1 \\ 0 & 1 \end{pmatrix} \begin{pmatrix} \cos\left(l_{p,\mathrm{SL}}\sqrt{k}\right) & \sin\left(l_{p,\mathrm{SL}}\sqrt{k}\right)/\sqrt{k} \\ -\sqrt{k}\sin\left(l_{p,\mathrm{SL}}\sqrt{k}\right) & \cos\left(l_{p,\mathrm{SL}}\sqrt{k}\right) \end{pmatrix} \begin{pmatrix} 1 & 1 \\ 0 & 1 \end{pmatrix} \tag{79}$$

$$= \begin{bmatrix} \cos\left(l_{p,\mathrm{SL}}\sqrt{k}\right) - \sqrt{k}\sin\left(l_{p,\mathrm{SL}}\sqrt{k}\right) & \left[\frac{1}{\sqrt{k}} - \sqrt{k}\right]\sin\left(l_{p,\mathrm{SL}}\sqrt{k}\right) + 2\cos\left(l_{p,\mathrm{SL}}\sqrt{k}\right) \\ -\sqrt{k}\sin\left(l_{p,\mathrm{SL}}\sqrt{k}\right) & \cos\left(l_{p,\mathrm{SL}}\sqrt{k}\right) - \sqrt{k}\sin\left(l_{p,\mathrm{SL}}\sqrt{k}\right) \end{bmatrix} \tag{80}$$

We can do the same again, letting the elements on the diagonal equal to -1. Inserting the plasma lens radius $l_{p,\mathrm{SL}}$, we get the plasma lens strength to be

$$k = 3.69\ 1/\mathrm{m}^2 \tag{81}$$

We see that the plasma lens strength here is similar to the thin lens approximation, $4/\mathrm{m}^2$, which is a good sign. We insert the calculated lens strength in the formula for the plasma lens strength, Eq. 15, and solve for the corresponding current I_p for such a lens.

$$I_p = \frac{2E\pi R_p^2 k}{ec\mu_0} \tag{82}$$

$$\Rightarrow I_{p,SL} = 9.50\,\mathrm{kA} \tag{83}$$

The current for the thin lens approximation, will similarly be 10.3 kA. We have in other words a relative difference of 8.5%. We can look at the Acceptance map and final phase space, if we use this single lens compared to the multiple lens configurations above. We should get a mirror of the initial phase space, as long as $x << x'$.

This seems to not be the case if we look at both the Acceptance map and the final beam in Fig. 21 and Fig. 22 respectively. We see that the Acceptance Map seems to only depend on a given α, while we observe the same phase space as in Fig. 18 in the phase space, only rotated by an angle.

It seems our theoretical results for thin lenses are similar to that with the thick lenses. We will not manage to refocus α with this design, since the transverse positions can not be said to be from a point source. If we then calculate the final beam values, we see exactly this

$$\sigma_{x,\mathrm{SL}} = 104\ \mu\mathrm{m} \tag{84}$$

$$\epsilon_{x,\mathrm{SL}} = 0.0149\ \mathrm{mm\ mrad} \tag{85}$$

$$\alpha_{x,\mathrm{SL}} = -1.46\ \mathrm{m} \tag{86}$$

$$\beta_{x,\mathrm{SL}} = 0.725\ \mathrm{m} \tag{87}$$

$$N_{SL} = 100\% \tag{88}$$

The thick lens have kept the deviations of the particle positions, but not for the transverse momenta. The core would still be focused correctly, since we have a small difference of transverse position here. We can see this in Fig. 22; the core is only rotated by an angle, and have not changed form.

4. Conventional quadrupoles

For comparison, we should also look at the case with conventional quadrupole instead of plasma lenses. Here we shall only focus only in one transversal dimension. Since quadrupoles has no axzially symmetric focusing effect, as the plasma lens has, the total length for a quadrupole lattice will necessarily be longer than the result here. It is therefore only a lower limit, an indication of the amount of space we definitely need.

We use the quadrupoles of similar order as used in the CLIC test-facility [25], letting the gap between each quadrupole to be as long as the quadrupoles themself. Resulting parameters to find the lower limit for conventional quadrupoles are then:

$$L_q = 1\ \mathrm{m} \tag{89}$$

$$g_q = 100\ \mathrm{T/m} \tag{90}$$

$$R_q = 10\ \mathrm{cm} \tag{91}$$

We do the same trick again for the two quadrupoles in the middle, change the length such that we have $\alpha = 0$ between them. We end up needing 8 quadrupoles, where the two quadrupoles in the middle will have a length of around 62 centimeters. This will give

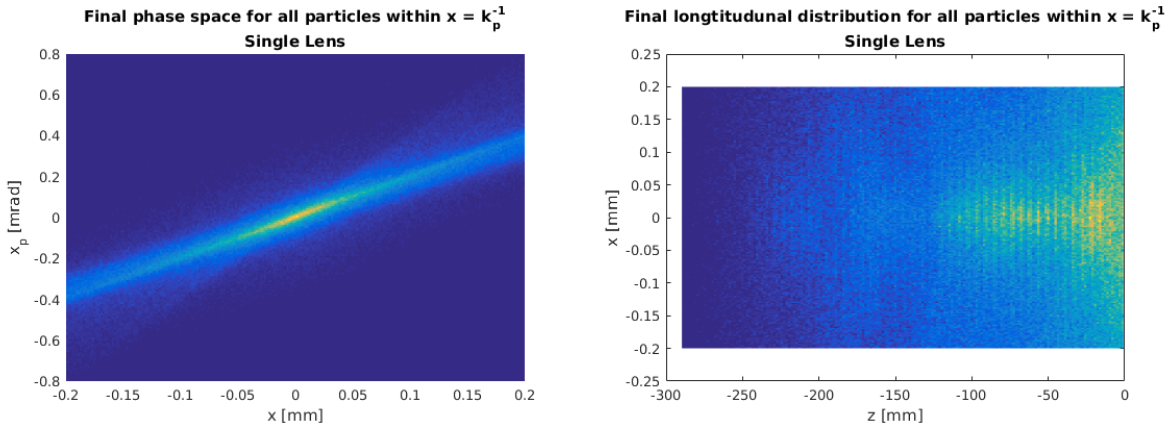

FIG. 22: The final beam after a single high current lens, $s = 1.5$ meters of beam line. On the left the phase space is plotted, while on the left we see the final longitudinal distribution. The limits on the axes are from the initial beam in Fig. 14. We observe a rotated phase space compared to the initial phase space, but the longitudinal distribution seems to be similar.

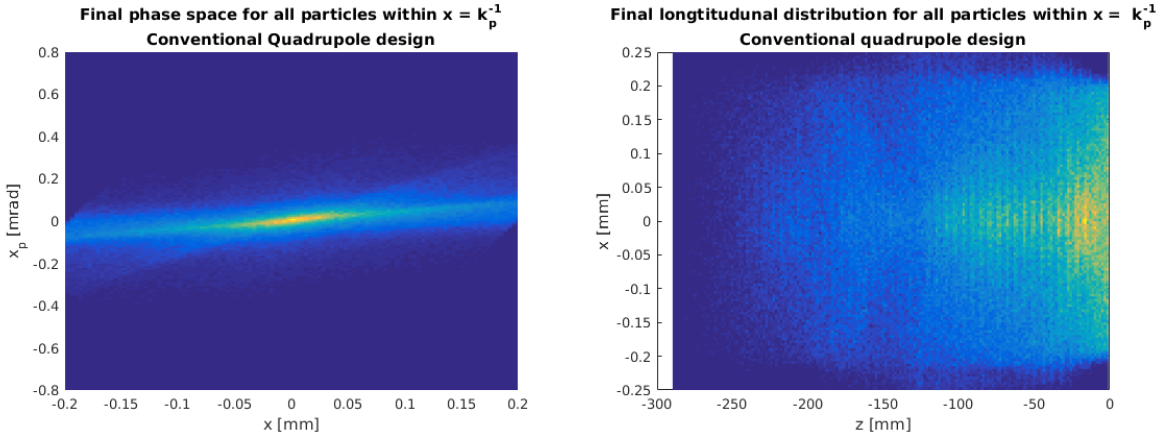

FIG. 23: The final beam when we used quadrupoles instead of plasma lenses, resulting in total a beamline of length $s = 17$ meters. On the left the phase space is plotted, while on the right we see the final longitudinal distribution. The limits on the axes are again from the initial beam in Fig. 14.

---

in total 17 meters, and a phase space as shown in Fig. 23.

If we instead had calculated to get $\alpha = 0$ in the middle of a quadrupole, we could probably reduce this length by a few meters. We can for this design also calculate how the beam has evolved right before we enter the plasma cell for plasma wakefield acceleration. We have here

$$\sigma_{x,q} = 105\ \mu\text{m} \tag{92}$$

$$\epsilon_{x,q} = 0.0149\ \text{mm mrad} \tag{93}$$

$$\alpha_{x,q} = -0.420\ \text{m} \tag{94}$$

$$\beta_{x,q} = 0.744\ \text{m} \tag{95}$$

$$N_q = 100\,\% \tag{96}$$

The only difference from the designs with multiple lenses is a very different α, while other numbers are very similar to that of the initial cut beam.

C. Nonlinearity considerations

As dicussed in Section II B 1, magneto-hydrodynamics simulations [13] show that active plasma lenses are expected to have a nonlinear component of the magnetic field due to nonuniform current density. In this section we investigate how the expected nonlinearities are affecting the performance of the interstage discussed previously (where linear fields were used).

We apply the nonlinear focusing term, expressed by Eq. 16 to the interstage designs discussed above. We then found this current density by solving for the heat flow equation,

$$\frac{d^2u\left(x\right)}{dx^2}+\frac{1}{x}\frac{du\left(x\right)}{dx}=-u\left(x\right)^{3/7} \tag{97}$$

where x is the ratio of r to R_p. This can the be inserted into $T_e = Au^{2/7}$, using the same numerical constants as in the paper[13], mainly by $u_0 = 0.087$ in the center of the lens. We then used the current distribution to get a set of sorted bins for the azimuth magnetic field gradient, as defined in Eq. 14.

We then sorted the beam in absolute value of r, and focused each bin by a corresponding gradient in that range (from 0 to R). The current was changed such that the gradient at the center of the plasma lens was the value from the uniform current, giving a decrease of 35.7%.

For all interstage designs, the nonlinear situation will not change β drastic, while α will increase in for the multiple lens design. For the single lens the opposite is the case for α when we introduce nonlinearities, here a single high current lens will have a much better preserved beam, as shown in Table VI.

We can also see this effect is we look at the acceptance map for the lattice designs for multiple plasma lenses. The nonlinear version of these are shown in Fig. 24, to be compared to Fig. 17 and 20 respectively. It seems that the constraint on the transverse momenta has been lowered, while the the accepted positions has increased instead. The cross-section has however sunk, and this explain the loss of more particles when we include the nonuniformity of the current.

We see from Table VI, that the survival as decreased by 10% if we use more than one plasma lens. Probable are these the particles at the outer phase space, and not the core of the beam. While the survival rate and α are not affected a lot by the nonlinearity for both the initial and short design, this is not the case for β and the self-modulation. Similarly for the single lens, the bunch size will increase with nonlinearity. This is easily understood, the particles outside the core are influenced by a weaker magnetic field, and are therefore not focused enough.

The opposite is the case for the inner core, which can explain why the degree of self-modulation will not be preserved when we introduce nonlinearity. In both cases with multiple lenses the degree of self-modulation is halved. This is a bit better when we uses fewer plasma lenses in the short design, while for a single high current lens the difference is not that drastic. It seems that an increased plasma lens length will not improve the result by much.

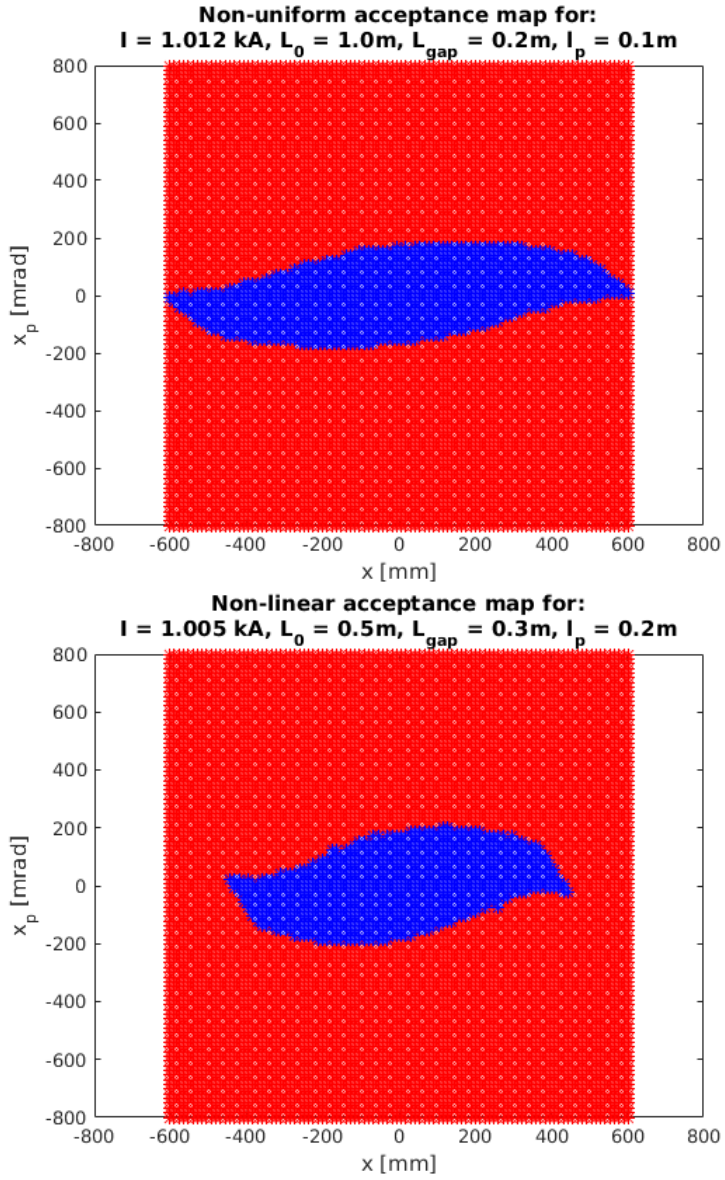

FIG. 24: The acceptance map for both designs with multiple lenses, initial and the short design. Here we have taken into account nonlinearity. They should be compared to the acceptance maps in Fig. 17 and 21 respectively. We observe that that accepted transverse momenta has been reduced.

TABLE VI: All the configurations with nonlinear consideration. The first two are the multiple lens configurations from Table V, and the single lens from the calculation above. Included is a focusing lattice with quadrupoles for comparison. The relative changes are calculated in relation to the initial values in Eq. 47-50. Only the short design and the single lens are within ten meters. We also see that when we include nonlinearities, the designs with multiple plasma lenses will not preserve the self-modulation.

Configuration	Initial Design	Short design	Single lens	Quadrupoles
Current I_p	1.012 kA	1.005 kA	9.502 kA	None
Max radius R_p	1.604 mm	0.9759 mm	0.6251 mm	10 cm
Lenses/Quads needed	58	20	1	8
Total length s	19.2 m	10.7 m	1.5 m	17 m
Survival (uniform fields)	94.2%	94.0%	99.1%	100%
Survival (nonlinear fields)	80.9%	83.0%	99.1%	100%
Relative change β	0.233	0.136	0.001	0.217
Relative change β (nonlinear)	2.37	1.59	0.185	0.217
Relative change α	1.01	0.737	-5.55	- 2.97
Relative change α (nonlinear)	1.29	0.846	-2.16	-2.97
Self-modulation N	100%	100%	100%	100%
Self-modulation N (nonlinear)	56.9%	62.2%	97.9%	100%

V. DISCUSSION AND CONCLUSIONS

Let us the recap the problem in this thesis. Since we need to self-modulate the proton beam before the acceleration stage, we need two separate plasma cells in the AWAKE beam line. This creates a gap between them, the interstage, where we need to refocus the proton beam again. The gap length should be as short as possible, due to limited space in the experimental area. Regular magnetic quadrupoles do not give a satisfactory solution. Is it possible to use active plasma lenses instead, while still preserving the quality of the proton beam?

While plasma lenses do have several advantages compared to quadrupoles, mainly axisymmetric focusing and possibilities for very high gradients, the plasma nature in itself creates new challenges. We have looked at two different sources of nonlinearity in this thesis:

- Nonlinearity from the induced wakefield of the charged beam itself
- Nonlinearity from a non-uniform current in the plasma lens

A. The effects of wakefield in plasma lenses

The wakefield he wakefield depends on the parameters of the charged beam passing through the lens. The effect can be estimated using linear theory. As part of an Oslo-experiment to further quantify the effect of wakefields at the CLEAR test-facility at CERN, we performed extensive wakefields calculations for CLEAR.

For the experiments at CLEAR itself, we found that we will be able to both measure the situations where wakes will have a significant effect or not on the beam.
We also verified our calculations of linear wakefield theory with a 3D particle-in-cell code, QuickPIC. While the PIC results at towards the boundaries were not fully conclusive due to noise that were not fully understood, the results close to the axis, which is our region of interest, show excellent correspondence with the linear theory.

We also used QuickPIC to verify and confirm that the beam would not focus and significantly modify the wake as the beam propagates through the plasma lens, giving

further confidence in our linear wake calculations.

The linear wake calculations were finally applied to the case of the AWAKE proton beam. We found that for a plasma lens within 1 millimeters, we can neglect the wakefields entirely.

B. Lattice designs for the AWAKE interstage

We looked at different designs for the interstage to see whether the plasma lenses are worth to use instead of quadrupoles. We ended up with four different solutions,

- A design with the lenses of today, totaling up to 19 meters
- A possible design with better, longer lenses, which reduced the beam line to 11 meters
- A single high current lens instead,
- And an estimate for how long a quadrupole design would be, to at least 17 meters

The initial design and the short design give nearly the same result when we look at the relative change of phase space as well as the amount of particles surviving the lattice. However there are problems with the plasma lenses that are only ten centimeters long, we ended up with twice the length compared to a future possible design. The number of lenses are also probably too much to be worth it, especially when many of these lenses has a radius over 1 millimeters. We will therefore have problems with wakefields as well for this design.

How did we fare if we only increased the current instead, by an order of magnitude? While the plasma lens radius and the total beam line length are good, we do however have some problems with the beam itself. While we assumed a situation where the transverse position could be assumed smaller than the momenta, this is not the case here. We can see this for how the relative change for α is way off compared to all other designs, even for the quadrupole design. There are however one thing it improves from the lattice with multiple lenses, the survival rate have increased.

It seems that the survival rate will not change much after the first plasma lenses, and it seems that we get a better beam quality if we increase the current than the plasma lens. If we then increased the current for the short design with future, probably plasma lenses, we could then decrease the total length as well as the survival rate would increase since the number of lenses needed would decrease.

C. Nonlinearities from non-uniform current

We then replaced the model with a radially uniform current by a more realistic model based in magneto-hydrodynamic simulations. From the acceptance map, we see that this change will reduce the highest possible transverse momenta. The reduction seems to be a constant relation regardless of the amount lenses or their length. So our argument that we need to use lenses with higher values than currently available for the AWAKE interstage seems still to hold.

When also taking the degree of self-modulation into account, this argument becomes stronger. The only designs that are affected by the non-linearity negatively are when we have multiple plasma lenses. In both these cases the degree of self-modulation are halved, while it is constant for the single lens design, since it has only one lens. It does not seem to depend strongly on the amount of plasma lenses, the difference between the two proposals are only a few percent.

D. Conclusion

The interstage between the two plasma cells at AWAKE for the second phase can't be longer than around ten meters, before we get problem either upstream or downstream. For all different options studied, only lenses based on improved technology with respect to today's state of the art are interesting. If we remove our assumption about uniform current, the improved lenses would not preserve the amount of self-modulation. While we could neglect the wakefields for the stronger plasma lenses, it seems that the only way to use plasma lenses for a focusing lattice is if we could increase the currently available current, as well as increasing their length. If a combination of these two improvements could be achieved, the plasma lenses could possibly be a solution for an AWAKE interstage.

References

[1] M. Koratzinos *et al.*, "TLEP: A High-Performance Circular e^+e^- Collider to Study the Higgs Boson," in *Proceedings, 4th International Particle Accelerator Conference (IPAC 2013): Shanghai, China, May 12-17, 2013* (2013) p. TUPME040, arXiv:1305.6498 [physics.acc-ph].

[2] Halina Abramowicz *et al.*, "The International Linear Collider Technical Design Report - Volume 4: Detectors," (2013), arXiv:1306.6329 [physics.ins-det].

[3] M Aicheler *et al.*, "A Multi-TeV Linear Collider Based on CLIC Technology," (2012), 10.5170/CERN-2012-007.

[4] T. Tajima and J. M. Dawson, "Laser electron accelerator," Physical Review Letters **43**, 267–270 (1979).

[5] M. Litos *et al.*, "High-efficiency acceleration of an electron beam in a plasma wakefield accelerator," Nature **515**, 92–95 (2014).

[6] A. Caldwell, K. Lotov, A. Pukhov, and F. Simon, "Proton-driven plasma-wakefield acceleration," Nature Physics **5** (2009), 10.1038/NPHYS1248.

[7] A. Caldwell and K. Lotov, "Plasma wakefield acceleration with a modulated proton bunch," Physics of Plasmas **18** (2011), 10.1063/1.3641973.

[8] W. K. H. Panofsky and W. R. Baker, "A focusing device for the external 350mev proton beam of the 184inch cyclotron at berkeley," Review of Scientific Instruments (1950), 10.1063/1.1745611.

[9] J. van Tilborg *et al.*, "Active plasma lensing for relativistic laser-plasma-accelerated electron beams," Physical Review Letters **115** (2015), 10.1103/physrevlett.115.184802.

[10] K. Greene and R. Kaltschmidt, "World record for compact particle accelerator," Berkely Lab (2014), [Online via http://newscenter.lbl.gov/2014/12/08/world-record-for-compact-particle-accelerator/].

[11] E.D Courant and H.S Snyder, "Theory of the alternating-gradient synchrotron," Annals of Physics **3**, 1–48 (1958).

[12] K. Wille, "The Physics of Particle Accelerators : An Introduction," (Oxford Univ. Press, 2000).

[13] J. van Tilborg *et al.*, "Nonuniform discharge currents in active plasma lenses," Phys. Rev. Accel. Beams **20**, 032803 (2017).

[14] Hans L. Pesceli, "Waves and Oscillations in Plasmas," (CRC Press, 2012).

[15] I. Blumenfeld, *Scaling of the longitudinal electric fields and transformer ratio in a non-linear Plasma Wakefield Accelerator*, Ph.D. thesis, Stanford University (2009).

[16] M.Brugger *et al.*, "The CLEAR facility at CERN," Technical Note CERN (2016), [Online via https://clear.web.cern.ch/sites/clear.web.cern.ch/files/documents/CLEAR_proposal.pdf].

[17] S. Steinke *et al.*, "Multistage coupling of independent laser-plasma accelerators," Nature (2016), 10.1038/nature16525.

[18] Weiming An, Viktor K. Decyk, Warren B. Mori, and Thomas M. Antonsen Jr., "An improved iteration loop for the three dimensional quasi-static particle-in-cell algorithm: Quickpic," Journal of Computational Physics **250**, 165 – 177 (2013).

[19] Erik Adli, "Towards AWAKE applications: Electron beam acceleration in a proton driven plasma wake," in *Proceedings of IPAC2016, Busan, Korea* (2016).

[20] E. Gschwendtner *et al.*, "AWAKE, the advanced proton driven plasma wakefield acceleration experiment at CERN," Nuclear Instruments and Methods in Physics Research Section A: Accelerators, Spectrometers, Detectors and Associated Equipment **829**, 7682 (2016).

[21] V.K.B. Olsen *et al.*, "Loading of a plasma-wakefield accelerator section driven by a self-modulated proton bunch," in *Proceedings of IPAC2015* (2015) pp. 2551 -2554.

[22] V.K.B. Olsen *et al.*, "Loading of wakefields in a plasma accelerator section driven by a self-modulated proton beam," in *Proceedings of NAPAC2016* (2016) in press.

[23] A. P. Sosedkin and K. V. Lotov, "LCODE: A parallel quasistatic code for computationally heavy problems of plasma wakefield acceleration," *2nd European Advanced Accelerator Concepts Workshop (EAAC2015) La Biodola, Isola d'Elba, Italy, September 12-19, 2015*, Nucl. Instrum. Meth. **A829**, 350–352 (2016).

[24] K. Lotov, "Physics of beam self-modulation in plasma wakefield accelerators," Phys. Plas **22** (2015), 103110.

[25] J. A. Clarke *et al.*, "Novel tunable permanent magnet quadrupoles for the CLIC drive beam," IEEE Transactions on Applied Superconductivity **24**, 1–5 (2014).